

1 **Lifetime fitness is correlated more strongly with structural variant than SNP mutational**
2 **load in a threatened bird species**

3

4 Katarina C. Stuart^{1,2*}, Hui Zhen Tan¹, Annabel Whibley^{1,3}, Sarah Bailey¹, Patricia Brekke⁴, John G.
5 Ewen⁴, Selina Patel¹, Anna W. Santure¹

6 ¹ Ecology and Evolutionary Biology Group, School of Biological Sciences, University of
7 Auckland, Auckland, 1142, Aotearoa New Zealand

8 ² University of New South Wales, Sydney, Australia

9 ³ Bragato Research Institute, Blenheim, Aotearoa New Zealand

10 ⁴ Institute of Zoology, Zoological Society of London, London, UK

11 *Correspondence: Katarina.stuart@auckland.ac.nz

12 **Abstract**

13

14 The field of conservation genomics is becoming increasingly interested in whether, and how,
15 structural variant (SV) genotype information can be leveraged in the management of threatened
16 species. The functional consequences of SVs are more complex than for single nucleotide
17 polymorphisms (SNPs), as SVs typically impact a larger proportion of the genome due to their
18 size, and thus may be more likely to contribute to load. While the impacts of SV-specific genetic
19 load may be less consequential for large populations, the interplay between weakened
20 selection and stochastic processes mean that smaller populations, such as those of the
21 threatened Aotearoa hihi/New Zealand stitchbird (*Notiomystis cincta*), may harbour a high SV
22 load. Hihi were once confined to a single remnant population, but have been reestablished into
23 six sanctuaries and reserves, often via secondary bottlenecks, resulting in low genetic diversity,
24 low adaptive potential and inbreeding depression. In this study, we use whole genome
25 resequencing of 30 individuals from the Tiritiri Matangi population to identify the nature and
26 distribution of both SNPs and SVs within this small avian population. We find that SNP and SV
27 individual mutation load is only moderately correlated, likely because SVs arise in regions of
28 high recombination and that are less evolutionarily conserved. Finally, we leverage a long-term
29 monitoring dataset of pedigree and fitness data to assess the impact of SNP and SV mutation
30 load on individual fitness, and demonstrate that SV load correlates more strongly than SNP
31 load with lifetime fitness. The results of this study indicate that only examining SNPs neglects
32 important aspects of intraspecific variation, and that studying SVs has direct implications for
33 linking genetic diversity and genomic health to inform management decisions.

34 **1 | Introduction**

35

36 Inclusion of genomic data into conservation management is becoming more common practice.
37 For wild unmanaged species and populations, this is being driven by the increasing recognition
38 of the ability of genomic data to reveal many biologically relevant patterns within species, such
39 as cryptic information about animal dispersal (Alves et al., 2023), demographics (Zhao et al.,
40 2013), and local adaptation (Yang et al., 2016), which may provide valuable information to guide
41 population delineations and management practices. For species undergoing more active
42 management such as breeding programs, assisted translocation, and genetic rescue, genomic
43 data is essential to facilitate optimal conservation outcomes. These data allow for
44 quantification of inbreeding levels (Hedrick et al., 2016), assessing the impacts of deleterious
45 mutations (Humble et al., 2023), and monitoring the outcomes of breeding programs
46 (Frankham, 2008; Lynch & O’Hely, 2001), which may greatly impact the long-term survival of a
47 population of interest.

48

49 As conservation managers increasingly incorporate genomic data into practice, there is growing
50 discussion around the relative utility of different genomic sequencing approaches (Theissinger
51 et al., 2023). Amongst these is whole genome resequencing (WGR), which involves sequencing
52 of the entire genomic DNA present within an organism. Despite a steady decrease in
53 sequencing costs over recent decades, WGR may still be prohibitively expensive for population-
54 level sequencing in many systems (Fuentes-Pardo & Ruzzante, 2017). WGR has been primarily
55 applied in the study of health (Turro et al., 2020), model organism systems (Cao et al., 2011)
56 and for agriculturally important species (Usha et al., 2022), however its application in wild
57 populations has been gaining popularity. Application of WGR data to conservation genomics
58 has revealed that while WGR may reflect the same broad patterns seen in more economical
59 approaches (Duckett et al., 2023), the high density of genetic markers is invaluable for some
60 genomic analysis such as inferring the landscapes of inbreeding (Duntsch et al., 2021) and
61 genomic divergence (Szarmach et al., 2021). An important question then remains of whether,
62 given this extra cost, WGR has unique utility to conservation biology practice, and if so, under
63 what set of circumstances (Fuentes-Pardo & Ruzzante, 2017; Haig et al., 2016; Kardos et al.,
64 2021; McMahon et al., 2014).

65

66 One area in which WGR plays a vital role is in the profiling of complex genomic variants,
67 including structural variants (SVs), alongside single nucleotide polymorphisms (SNPs) (Kardos

68 et al., 2021). SVs typically span tens of bases to multiple megabases (Scherer et al., 2007), and
69 are increasingly being recognised as important components of intra-specific genetic variation
70 (Catanach et al., 2019; Wellenreuther et al., 2019; Wold et al., 2023). The functional
71 consequences of SVs may be more complex than for single nucleotide polymorphisms (SNPs),
72 as SVs typically impact a larger proportion of the genome (Collins et al., 2020), may harbour and
73 accumulate SNPs and other small genetic variants within their length (Mahmoud et al., 2019),
74 and are more likely to be deleterious when compared to SNPs (Hämälä et al., 2021).

75

76 To this end, the field of conservation genomics is becoming increasingly interested how SV
77 genotype information should be leveraged in the management of threatened species.
78 Population-level profiling of genome-wide SVs require a minimum of moderate depth short-
79 read WGR data, though they still remain technically challenging to identify (Mahmoud et al.,
80 2019). The SVs may not be in strong linkage disequilibrium with the SNPs around them (Pang et
81 al., 2010), so it is not guaranteed that focal structural variants can have their genotypes inferred
82 from neighbouring or overlapping SNPs. Examining SNPs alongside SVs has revealed instances
83 where patterns in one type of genetic variation are not reflected in the other (Catanach et al.,
84 2019; Stuart et al., 2023). Ongoing research into intra-specific structural variants is continuing
85 to demonstrate the important role they play in, for example, facilitating convergent adaptation
86 (Kreiner et al., 2019), and revealing previously hidden genotype associations (e.g. environment
87 (Y. Li et al., 2024) or phenotype (Ruigrok et al., 2022)). Thus, the use of WGR data is essential to
88 provide a holistic representation of genome wide patterns of genetic diversity or to identify
89 specific variants associated with an ecotype or deleterious/beneficial functional trait.

90

91 One pressing area of research is the relative impacts of SNP and SV variants within small
92 populations, particularly in relation to concepts like inbreeding and genetic mutational load
93 (the accumulation of deleterious variants) (Hohenlohe et al., 2021). In small populations, novel
94 variants arise at initially higher frequencies and then may increase in frequency through drift.
95 Conversely, in large populations novel variants arise at a low frequency and the change in
96 frequency of the variants depend on the selection pressures present (Lohmueller, 2014).
97 Because SVs are less likely to be neutral than SNPs, we may expect that the weakened
98 selection within small populations (Edmonds et al., 2004) has the potential to produce
99 differential patterns in these two different types of variants. Understanding how genetic
100 mutational load, might differ when quantified using SNPs and SVs will be vital for linking

101 underlying patterns of genetic diversity to functional traits related to individual fitness,
102 population persistence, and adaptive potential.

103

104 Characterising genetic load is particularly relevant in threatened species, such as those of the
105 hihi/stitchbird (*Notiomystis cincta*) (Fig. 1a). This species once covered much of Aotearoa New
106 Zealand's North Island, but their natural range had been reduced to a single offshore island, Te
107 Hauturu-o-Toi by the 1880s (Fig. 1a; Brekke et al., 2011). This single remnant population has
108 been used to establish a primary breeding colony on the offshore island of Tiritiri Matangi
109 (Miskelly & Powlesland, 2013), from which most additional populations have been
110 reestablished or supplemented (Brekke et al., 2011). However, the long-term success of
111 established populations has been variable, with some experiencing limited population growth
112 post-founding, and others failing to establish (Ewen et al., 2013; Parlato et al., 2021). While
113 population success is dependent in part on extrinsic factors (e.g. Doerr et al., 2017), inbreeding
114 and low adaptive potential within the species are also likely to be contributing to poor
115 population health (de Villemereuil et al., 2019; Duntsch et al., 2023). The Tiritiri Matangi
116 population is intensively monitored, including recording pedigree information and lifetime
117 fitness, and so the hihi provides a means to better understand the differential impacts of SNP
118 and SV genetic load on important conservation metrics such as fitness.

119

120 In this study, we use whole genome resequencing of hihi individuals from the Tiritiri Matangi
121 population to identify the nature and distribution of both SNPs and SVs within this small avian
122 population. We quantify mutation load and assess how well individual SNP load acts as a proxy
123 for SV load. We also examine the genomic location of SVs with respect to underlying patterns of
124 recombination and avian genomic evolutionary conservation, to better understand how SVs
125 arise and are maintained within the genomes of a species. Finally, leveraging a long-term
126 monitoring dataset of fitness data for each individual, we test the impact of SNP and SV
127 mutation load on lifetime fitness. We hypothesise that relative patterns in these two types of
128 variants will reveal that SVs have a greater impact on lifetime fitness, reflecting the more
129 deleterious nature of SVs in comparison to SNPs.

130

131 **2 | Methods**

132 **2.1 | Sampling**

133 We selected a total of 31 hihi (*Notiomystis cincta*) individuals for inclusion in the study. These
134 individuals comprise four hihi sampled from the remnant population on Te Hauturu-o-Toi / Little
135 Barrier Island, Aotearoa / New Zealand (36°12' S, 175°05' E) and 27 sampled from the
136 reintroduced population on the island of Tiritiri Matangi (36°36' S, 174°53' E) (Fig. 1a). Of the four
137 Te Hauturu-o-Toi individuals, two were translocated to Tiritiri Matangi in 2010 as a genetic
138 rescue attempt (Nichols et al., 2024), both of which successfully bred in the population. The
139 remaining two were sampled in 2017 and 2018 as part of a population diversity survey on Te
140 Hauturu-o-Toi and were subsequently selected as our reference male and reference female for
141 genome assembly (Bailey et al., 2023). Individuals on Tiritiri Matangi were sampled in several
142 cohorts from 2001-2011 and were chosen as individuals that successfully bred and therefore
143 are likely to represent diversity present in the current population. We note that because many
144 hihi individuals do not breed successfully, this study assesses how load impacts the level of
145 reproduction in known breeding individuals, rather than whether load impacts the occurrence
146 of successful breeding. Blood samples were taken at capture of all individuals via brachial
147 venepuncture and stored in 95% ethanol. All individuals have been previously genotyped at a
148 panel of 20 microsatellite markers (Brekke et al., 2009), which enables genetic sexing of the
149 birds alongside inclusion in a genetically resolved pedigree for the entire Tiritiri Matangi
150 population. The dataset includes 17 females, 14 males, and three close family groups; a parent-
151 offspring duo, a half-sibling pair and their genotyped father, and eleven focal individuals
152 connected in a multi generation family, which includes two parent-offspring trios and four
153 further parent-offspring duos (family groups noted in Table S1).

154 We extracted gDNA from the blood samples of the 31 individuals with a Qiagen DNeasy Blood
155 and Tissue Kit. Library preparation and whole genome resequencing (WGR) was conducted by
156 AgResearch, New Zealand, in two experiments; in the first, libraries were prepared for
157 sequencing with an Illumina kit, in the second with a Nextera XT library preparation that reduced
158 adaptor contamination apparent in the first run. All samples (Table S1) were resequenced on
159 the Illumina NovaSeq 6000 platform with S4 flowcells (150 bp paired end reads).

160 **2.2 | Single nucleotide polymorphism calling**

161 We merged raw reads across the two experiments. We then used TRIM_GALORE v0.6.7 (Krueger,
162 2021) to process the merged reads using default settings and the flags '--paired' for paired reads

163 and ‘--fastqc’ to produce read quality reports that were then compiled and assessed with
164 MULTIQC v1.13 (Ewels et al., 2016). We mapped these processed reads to the female *N. cincta*
165 genome assembly version (Bailey et al., 2023) using the mapping algorithm BWA v0.7.17 (H. Li,
166 2013) *mem*. We used SAMTOOLS v1.16.1 (H. Li et al., 2009) to process the output files into sorted
167 BAM files, before marking duplicate reads within each file using PICARD v2.26.10 (*Picard Toolkit*,
168 2019) *MarkDuplicates*. Variants were then called using the program BCFTOOLS v1.13 (Danecek et
169 al., 2021), first using the *mpileup* (-C 50 -q 20 -Q 25) function to generate genotype likelihoods
170 and coverage information, then the *call* (-f GQ) function to produce SNP calls, *view* (--exclude-
171 types indels) function to retain only SNPs, and finally the *sort* function to order the SNPs into
172 chromosome and positional order. We filtered the remaining variants using VCFTOOLS v0.1.15
173 (Danecek et al., 2011) to retain only bi-allelic SNPs (--max-alleles 2) with a minimum depth of 5
174 (--minDP 5) and a maximum mean depth of 100 (--max-meanDP 100), removing non-variant
175 sites (--mac 1) and sites exceeding a missingness of 10% (--max-missing 0.9). We also filtered
176 out all Z and W chromosome contigs, and excluded one individual that had very high
177 heterozygosity estimates most likely due to sample contamination (individual 83318;
178 contamination was apparent from both sequencing experiments). Our total dataset was
179 therefore 30 birds, 26 of which were from Tiritiri Matangi and 4 of which were from Te Hauturu-o-
180 Toi.

181 **2.3 | Structural variant identification**

182 In order to identify the SV content within the 30 hihi individuals, we reanalysed the duplicate-
183 marked WGR data using the three short-read SV calling programs SMOOVE v0.2.8
184 (<https://github.com/brentp/smoove>), which is a wrapper for LUMPY-SV (Layer et al., 2014), DELLY
185 v0.8.2 (Rausch et al., 2012), and MANTA v1.6.0 (X. Chen et al., 2016). Calling SVs is based on
186 several lines of evidence produced by sequence data, including read depth and coverage, as
187 well as the mapping patterns of read-pairs and split-reads to infer the existence of a SV relative
188 to the reference genome. Identifying SVs from read data may contain many false positive calls
189 (Chakraborty et al., 2019; Weissensteiner et al., 2020; Wold et al., 2023), and thus often a
190 consensus approach is used where a particular variant is only retained if it is identified using
191 two independent variant caller programs. Specifically for this study, we chose to retain only SVs
192 that, after passing the individual program’s quality filters, were found in a minimum of two out of
193 the three variant calling programs used above. Briefly below we describe the three programs
194 and the quality filtering criteria used to exclude low quality SV calls.

195 We identified SVs using the program SMOOVE by following the population-level calling workflow
196 recommended in the program manual. This approach involves a per-individual variant calling
197 step where SVs are identified within each sample independently. The individual's SV calls are
198 then combined into one merged cross-sample SV list, which are then genotyped within each
199 individual separately before being combined again into a dataset containing all individuals. We
200 also included the optional annotation step, which uses the exon and untranslated region (UTR)
201 information in the genome annotation matching the *N. cincta* reference assembly to assign
202 quality scores to genotyped variants. Using these quality scores, we filtered deletions (DEL) to
203 $FMT/DHFFC < 0.7$, duplications (DUP) to $FMT/DHBFC > 1.3$, and all genotypes to $MSHQ \geq 3$,
204 following Wold et al. (2023), while also only retaining variants on autosomal chromosomes.

205 SVs were identified using the program DELLY by following the recommended germline SV calling
206 workflow. The workflow is similar to that used by SMOOVE, and involves a per-individual SV
207 calling step (*DELLY call*), a cross-sample SV calling merge step (*DELLY merge*), a per-sample
208 genotyping step (*DELLY call*) and finally a cross-sample SV genotype merging step which
209 combines all the individual SV calls into one variant file (*BCFTOOLS merge -m id*). We then filtered
210 the resulting variant calls to retain only those where a minimum of 50% of individuals were
211 assigned a per-individual 'PASS' score on their genotype, while also only retaining variants on
212 autosomal chromosomes.

213 We identified SVs using the program MANTA by following the default pipeline, which involved
214 using *configManta.py* to generate and run the MANTA workflow. We ran the initial variant file
215 through the MANTA function *convertInversion.py* in order to extract inversions (INV) from
216 breakend calls, which is not automatically done by the program. We then filtered variants using
217 *BCFTOOLS view*, retaining only those variants that were assigned a per-variant 'PASS' score, while
218 also only retaining variants on autosomal chromosomes.

219 We generated the consensus variant list using the program SURVIVOR v1.0.7 (Jeffares et al.,
220 2017), which merged the SVs identified by each program using several criteria, including the
221 maximum allowed distance between predicted breakends of 1 kb, two SV caller support needed
222 to retain a call, that the type and strand of the SV must agree, and a minimum SV length of 30 bp
223 (parameter values set as "1000 2 1 1 0 30"). Merging was done separately for each individual,
224 and we also forced SURVIVOR to only merge SV calls that agreed on genotype by merging
225 independently for homozygous reference, heterozygous, and homozygous alternate SV calls
226 within samples. Finally, we merged the retained variants into a joint sample file using the

227 parameters “1000 1 1 1 0 30” (setting the minimum SV caller support to 1 to create a merged
228 variant file).

229 **2.4 | Structural variant curation and validation**

230 The SURVIVOR consensus SV list was then filtered to only include deletion (DEL), duplication
231 (DUP) and inversion (INV) calls, as these were the three variant types that all three SV calling
232 programs could identify. We also removed large variants (>50,000 bp) and those with >50%
233 missing data across the 31 individuals. We also removed any SV that had no heterozygous
234 individuals, as it is unlikely that a polymorphic SV would exist without heterozygous individuals
235 being present. Similarly to SNPs, we also removed a contaminated sample from the dataset at
236 this step (individual 83318).

237 We manually curated these SVs to exclude false variants by visualising the raw sequence reads
238 across the identified SV loci for two individuals of each genotype (homozygous reference,
239 heterozygous, and homozygous alternate) where available. The visualisation was produced
240 using SAMPLOT v1.3.0 (Belyeu, Chowdhury, et al., 2021) and then scored using PLOTCRITIC v1.0.1
241 (Belyeu et al., 2018) by one curator to check for signals of SVs in the sequencing read depth and
242 insert sizes (Fig. S1-S6).

243 Because the Tiritiri Matangi population is small (~200 adults, Parlato et al., 2021), its pedigree is
244 highly connected, and as noted above, our data contained several related individuals, with over
245 half of the dataset organised into three family groups. Of these family groups, the large multi-
246 generation family included two parent-offspring trios with all three individuals resequenced. We
247 did not remove relatives from the dataset, but did use them to assess genotyping error rates and
248 to validate our manual curation. The program PLINK v1.09b6.16 (Purcell et al., 2007) was
249 employed to calculate Mendelian error rates using the two WGR trios using the ‘--mendel’ flag.
250 We assessed Mendelian error rates before and after manual curation, using both the two true
251 parent-offspring trios, as well as two fake trios. Mendelian error rates reported were the
252 averages of the two offspring individual error rates, which were each calculated by counting the
253 number of Mendelian errors present in the offspring divided by the total number of genotyped
254 sites within the offspring.

255 **2.5 | Structural variant filtering and profiling**

256 Some of the inter-individual variants detected by the above structural variant workflow will be
257 due to TE activity which has a different impact profile to SVs (Stuart et al., 2024). In this study we
258 are seeking to examine SV signals only, and hence removed any SV variants that had likely

259 resulted from TE activity (for further discussion on this see section 4.4: Technical validation of
260 SVs and exclusion of TEs). For this we ran REPEATMASKER v4.1.0 (Smit et al., 2013) on the SV
261 breakends (+/- 30 bp) using the *N. cincta* repeat library (Bailey et al., 2023), as repeat
262 identification in the genomic region around a breakpoint will allow for identification of variants
263 that are really TEs, rather than true SVs that simply contain a TE signal within their length.

264 Variants that had been identified as a TE (classification: LINE, LTR, SINE, DNA) were removed
265 from the SV data set, and then this data was filtered in VCFTOOLS to remove any non-variant sites
266 (--mac 1) and variants with more than 50% missingness (--max-missing 0.5).

267 We used PLINK to run a pca (--pca) on both the SNP and SV data. In addition, we compared
268 heterozygosity based inbreeding (VCFTOOLS --het), minor allele site frequency spectra (PLINK --
269 freq), and per-variant genotype frequencies for SNPs and SVs. For these analyses and all others
270 in the paper, the minor allele was used as the alternate allele.

271 **2.6 | Quantifying mutational load**

272 We sought to quantify per-individual genetic load for both SNPs and SVs, to examine the
273 correlation between load calculated from these two different genetic marker types. We first
274 needed to identify the positioning of variants relative to protein coding regions, as traditionally
275 only variants close-to or overlapping coding regions are considered as contributing to load
276 (Smeds et al., 2024). For this we used the variant effect predictor program VEP v107.0 (McLaren
277 et al., 2016) to profile the impacts of the variants, and then quantified variants into one of four
278 classes, based on their positioning relative to coding sequences. This included 'Gene' (variants
279 occurring in exons), 'Intron' (variants occurring in introns), 'Up-/Down-stream' (variants <5kb up-
280 and down-stream of a protein coding region), with all remaining variants being classed as
281 'None'. Variants of the three classes 'Gene', 'Intron', and 'Up-/Down-stream' were considered to
282 be variants contributing to load.

283 We quantified per-individual mutational load as both masked load and realised load. Masked
284 load was quantified as the proportion of load contributing variants that were heterozygous.
285 Realised load was quantified as the proportion of load contributing variants that were
286 homozygous for the minor allele. Both load calculations were done separately for SNPs and SVs.
287 Unfortunately, no close species of the hihi has been whole genome resequenced, and
288 additionally SVs often occur in more species-unique regions of the genome (see Fig. 4 below)
289 which means the use of more distant relatives is likely to bias the polarisation of SVs compared
290 to SNPs. Therefore, polarising these data was not possible, and so we use minor allele here in

291 place of derived allele. We compared how well correlated per-individual load was across SVs
292 and SNPs, by performing two regressions between the two comparing masked, and then
293 realised load using the *lm()* function from the TIDYR package in R.

294 **2.7 | Recombination rates and linkage disequilibrium**

295 We next sought to examine the genomic distribution of SVs within hihi, specifically in relation to
296 underlying recombination rates. The relationship between SVs and recombination rates is a
297 complex one, as recombination can give rise to SVs (Carvalho & Lupski, 2016), however the
298 presence of large SVs may inhibit recombination (Morgan et al., 2017). As part of our quality
299 control of SVs, acknowledging the challenges of identifying large SVs from short read data, we
300 excluded all SVs larger than 50kb, so our SV dataset is on average small and therefore unlikely to
301 inhibit recombination. The dataset is therefore most likely representative of the recombination
302 landscape in which SVs are likely to arise. We therefore tested to see if regions of the genome
303 with SVs present had higher recombination rates, with recombination rates summarised across
304 500Mb regions of the genome based on the hihi linkage map developed from pedigree (36
305 families) and SNP chip (33,890 autosomal SNPs) data (Tan et al., 2024). We analysed this
306 separately across macro- (chromosomes 1-7, 1A) and micro-chromosomes (8-29, 4A) because
307 they have very different recombination rates (chromosomal classification as per Bailey et al.
308 2023). We identified that SVs were present in 450 of the 1,251 macrochromosome
309 recombination windows, and for 221 of the 562 microchromosome windows.

310 Additionally, we examined patterns of linkage disequilibrium decay around SVs and contrasted
311 these to those seen around SNPs. For this, we combined all SV and SNP markers into one file,
312 and assessed the linkage disequilibrium for the SVs to the surrounding variants using the
313 *vcftools* function `--geno-r2-positions`, specifying and assessing pairwise linkage disequilibrium
314 up to 10 Mb away (`--ld-window-bp 1000000`). We also assessed SNP linkage disequilibrium
315 decay using the same metrics, creating five random subset of 935 SNPs which were averaged.
316 Finally, in order to better understand how processes of variant creation and selection may be
317 differentially impacted by the genomic landscape of macro- and micro-chromosomes, we
318 assessed the minor allele frequency of SNPs and SVs that do and do not contribute to load.

319 **2.8 | Evolutionary conservation analysis on multiple whole-genome alignments**

320 Next, we sought to identify where load contributing SNPs and SVs were positioned within the
321 hihi genome, with respect to genomic conservation across other avian species. For this, we
322 examined the hihi genome alongside additional passerine species downloaded from NCBI

323 including *Eopsaltria australis* (GCA_034509425.1), *Passer domesticus* (GCF_036417665.1),
324 *Hirundo rustica* (GCF_015227805.2), and *Taeniopygia guttata* (GCF_003957565.2), with *Gallus*
325 *gallus* (GCF_016699485.2) as an additional species to serve as an outgroup. We used TimeTree
326 v5 (Kumar et al., 2022) to create a Newick tree for these species, and used REPEATMASKER to soft
327 mask all the genomes using the Aves lineage specific sequences. We then aligned these six
328 genomes using the program PROGRESSIVE CACTUS v2.7.2 (Armstrong et al., 2020). We used the
329 function *halAlignmentDepth* from the HAL v2.3 (Hickey et al., 2013) toolkit implemented in
330 PROGRESSIVE CACTUS to calculate per base genome alignment coverage of the hihi genome. This
331 reports the number of other species that successfully mapped to each base position of the hihi
332 genome. A genome alignment value of 0 is indicative of a region that did not align across other
333 species and is unique to the hihi genome relative to the other species examined. A genomic
334 alignment value of 5 indicates that that all the other species' genomes aligned and is
335 interpreted as a conserved region.

336 We examined the level of genomic alignment underlying the SNPs and SVs, across the four
337 classes of 'Gene', 'Intron', 'Up-/Down-stream', and 'None' that were identified during load
338 quantification. We used BEDTOOLS to identify the genomic alignment value for SNPs based on
339 their positioning, while for SVs we used the average of their first and last base pairs so that the
340 level of genomic alignment was based on their breakends and not their sequence identity. To
341 quantify the genomic alignment values of SNPs and SVs relative to the whole genome, we also
342 calculated average evolutionary conservation for all 'Gene', 'Intron', 'Up/Down-stream' and
343 'None' sites genome-wide.

344 **2.9 Impacts of lifetime fitness**

345 Finally, leveraging a long-term monitoring dataset of pedigree and lifetime fitness data, which
346 was available for 28 out of the 30 individuals used in this study (because 2 of the Te Hauturu-o-
347 Toi birds were translocated and bred on Tiritiri Matangi), we assessed the impact of SNP and SV
348 mutation load on lifetime fitness. Lifetime fitness was measured as the total number of banded
349 offspring of each individual across its lifetime, and therefore measures fitness across one life
350 cycle, from banding to banding (de Villemereuil et al., 2019).

351 We set lifetime fitness as the dependent variable and ran three separate linear mixed models for
352 SNPs and SVs each; one for realised load (i.e., minor allele homozygotes at load sites), one for
353 masked load (i.e., heterozygous at load sites) and one for common allele homozygotes,
354 quantified as the proportion of load contributing variants that were homozygous for the major
355 allele (i.e., the remaining proportion of genotypes). In each model, the SNP / SV load was

356 included as a fixed effect along with individual sex, and sampling cohort was included as a
357 random effect. To quantify the relative contribution of SNPs and SVs to load, we also ran a
358 further two models where we included both variant types as fixed effects for each respective
359 category of load (i.e., masked and realised). In both models, individual sex was again included
360 as a fixed effect, and sampling cohort a random effect. Linear mixed models were run in R using
361 the *lmer()* function in the package LME4 v 1.1-26 (Bates et al., 2015).

362 We sought to examine if the evolutionary conservation had an impact on load by following up
363 significant results from the above models, of which only masked SV load was found to be
364 significant. We partitioned the masked SV load contribution up into two components: those
365 variants which fell into evolutionary conserved regions (where the average evolutionary
366 conservation score of the two breakends averaged was four or larger), and the remaining
367 variants. We ran a final linear mixed model as above, with just these two components of masked
368 SV load, and with individual sex as a fixed effect and sampling cohort as a random effect.

369

370 **3 | Results**

371 **3.1 | SV characterisation and validation**

372 Across the three SV detection programs, DELLY identified the largest number of variants at
373 13,176 SVs, closely followed by MANTA AT 12,672 SVs, with SMOOVE identifying only 3,275 SVs
374 (Table S2). From these, a total of 2,991 variants were identified in at least two out of the three
375 programs and were retained after meeting consensus criteria.

376 After manual curation this number was reduced to 1,229. Mendelian inheritance error rates
377 decreased from 1.6% to 0.9% after manual curation. We found that the Mendelian inheritance
378 rates of the true parent-offspring trios were much higher than for the fake trios, which were
379 14.2% and 17.8% before and after manual curation respectively. Of these curated SVs, we
380 identified 40.42% of them that were annotated as a type of repeat (Fig. 1b). Specifically, 293 of
381 these were identified as SVs that were likely to be TEs, and these were removed from the final SV
382 dataset, leaving a total of 936 variants. Of the identified TEs, LTRs were the most common TE
383 class, followed by LINEs, with very few SINE or DNA transposons, reflecting the large proportion
384 of LTRs and LINEs in the hihi genome (Bailey et al., 2023). Profiling of the SV length distributions
385 pre- and post-TE filtering confirmed that TE associated peaks were removed during this filtering
386 step (Fig. 1c) and identified that a majority of them fell in the range of 50-150 bp in length.

387 The cumulative length of the final filtered SV dataset was 420,304 bps, which was
388 approximately one seventh of the coverage of the final filtered SNP data set that consisted of
389 3,111,629 SNPs. The PCA produced from SNPs and SVs were very similar to one another (Fig.
390 S7), which both identified the Te Hauturu-o-Toi individuals distinct from those captured on
391 Tiritiri Matangi. Additionally, individual heterozygosity based inbreeding metrics were well
392 correlated across the two datasets (R -squared = 0.6291; Fig. S8), indicating that the SV dataset
393 represented a collection of high confidence SVs.

394 The site frequency spectrum (SFS) of SNPs and SVs was very similar in showing very few rare
395 alleles (Fig. 1d). However, the alternate/minor allele for SVs was more numerous than for SNPs,
396 appearing as an increase in heterozygous genotypes compared to homozygous reference (Fig.
397 1e).

398 **3.2 | Mutational load**

399 The genome wide distribution of SNPs and SVs was overall fairly similar, and generally reflective
400 of genome proportions of coding and non-coding regions, with the majority of variants either
401 intergenic or within introns (Fig. S9). However, the proportion of variants of each type that were
402 found to fall in coding or near coding regions was larger for SVs than SNPs (Fig. 2a, $F_{7,232}=8056$,
403 p -value = <0.0001).

404 We calculated mutational loads for all 30 individuals in the study, and assessed how well load
405 metrics were correlated with one another, as well as with individual inbreeding. From the total
406 genome-wide SNPs and SVs, 1,694,577 (54.7%) and 548 (58.5%) respectively were identified as
407 within or close to genes and therefore contributing to load (Figure 2a). SV load and SNP load is
408 significantly correlated for both realised and masked load, with SV and SNP realised load being
409 more highly correlated (Fig. 2c, $F_{1,28} = 51.29$, p -value = <0.0001 , $R^2 = 0.6343$) than SV and SNP
410 masked load (Fig. 2b, $F_{1,24} = 23.59$, p -value = <0.0001 , $R^2 = 0.4379$). In general, levels of load in
411 SVs and SNPs were more similar for realised load, while masked load values were slightly higher
412 for SVs than SNPs.

413 **3.3 | Recombination rates and structural variants**

414 We identified that there was a positive association between recombination rate and the
415 presence of SVs (Fig. 3a). We found that this difference was most pronounced on the
416 microchromosomes, which in general had higher recombination rates even within regions
417 without a SV present. Additionally, we found that pairwise linkage disequilibrium was slightly
418 higher for SNPs than for SVs when examining linkage disequilibrium decay up to distances of 10

419 Mb (Fig. 3b). This pattern was more stochastic at smaller distances (<10kb), though the bin of
420 variants closest to the SV breakends did see much lower linkage disequilibrium R^2 values than
421 for SNPs (Fig. S10). We found that patterns of minor allele frequency within SVs and SNPs are
422 reversed when split by load contribution and across chromosome type (macro- or micro-) (Fig.
423 S12).

424 **3.4 | Evolutionary conservation**

425 The inter-species genome alignment was completed for five avian species alongside the hihi
426 genome (Fig. 4a). We found that 61.1% of the hihi genome was evolutionary conserved across
427 all the other avian species examined, as measured by at least four other species aligning to
428 these sites, while 4.9% of the genome's length did not align to any other species and is unique
429 to the hihi (Fig. S12). Patterns of genome conservation alignment were fairly consistent across
430 all the hihi's autosomal chromosomes, though the proportion that was conserved across all
431 species decreased as chromosome length also decreased (Fig. S12).

432 Genome wide patterns of genome alignment, which we use to benchmark patterns in SNPs and
433 SVs, found that gene regions were the most evolutionarily conserved, up- and down-stream
434 gene regions were the most unique, while intron and non-coding regions were similar (Fig. 4b).
435 This pattern was consistent in SNPs and SVs, with the only deviation being that SNPs had higher
436 levels of genomic alignment in the intron variants when compared to the variants that were not
437 within or near coding regions ('None'). The average level of genomic alignment for both SNPs
438 and SVs was lower than the genome-wide patterns (including both variant and non-variant
439 sites), though this decrease in genomic alignment was more pronounced in SVs. This pattern is
440 primarily due to an inflation of the number of SV breakends that occurred in evolutionarily
441 unique regions of the hihi's genome, in comparison to SNPs (Fig. S13).

442 **3.5 | Mutational load impact on lifetime fitness**

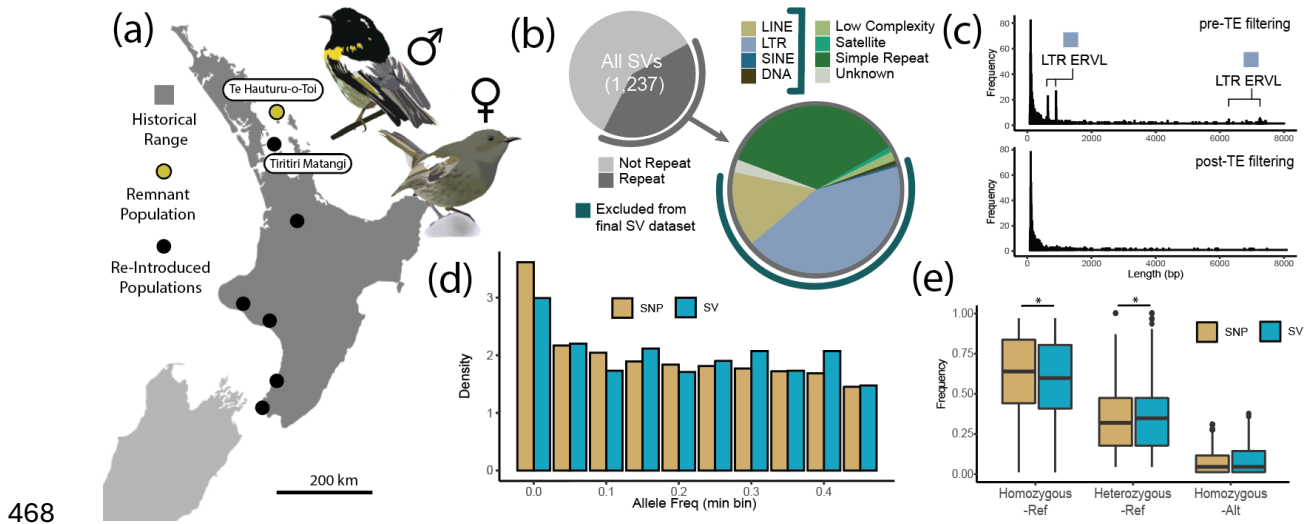
443 We found a significant negative relationship between both SNP realised load (Fig. 5a) and SV
444 (Fig. 5d) realised load with lifetime fitness (Table S3, $\beta = -235.988$, p-value = 0.0216 and $\beta = -$
445 232.252, p-value = 0.0126 respectively). Contrastingly, we found a positive relationship between
446 both SNP masked load (Fig. 5b) and SV masked load (Fig. 5e) with fitness, though SNPs had a p-
447 value just above the significance threshold (Table S3, $\beta = 168.152$, p-value = 0.0622 for SNPs
448 and $\beta = 218.218$, p-value = < 0.0001 for SVs). The contribution of common homozygote
449 genotypes at load sites was less consistent in the SNP and SV datasets, with SNP homozygosity
450 (Fig. 5c) not significantly correlating with fitness, while SV homozygosity (Fig. 5f) was negatively

451 and significantly correlated (Table S3, $\beta = 0.7033$, p-value = 0.9925 for SNPs and $\beta = -137.680$, p-
452 value = 0.0124 for SVs).

453 To determine the relative contribution of SVs and SNPs to the load signals, we ran a further two
454 linear mixed models, one fitting both SNP and SV masked mutational load, and one fitting both
455 SNP and SV realised mutational load. Within the masked load model, we found that masked SV
456 load was positively correlated with lifetime fitness (Table S3, $\beta = 250.698$, p-value < 0.0001),
457 however this trend was neither significant nor in the same direction for masked SNP load (Table
458 S3, $\beta = -81.899$, p-value = 0.3050). Within the realised load model, neither realised SV load
459 (Table S3, $\beta = -183.658$, p-value = 0.1893) nor realised SNP load (Table S3, $\beta = -65.136$, p-value =
460 0.6680) was significantly associated with lifetime fitness, though both trends were consistently
461 negatively associated with lifetime fitness.

462 We partitioned the SV masked load into evolutionary conserved and less conserved genomic
463 regions and found that both these components of masked SV load were significantly and
464 positively correlated with lifetime fitness (conserved regions: $\beta = 233.937$, SE= 67.190, t-value =
465 3.482, p-value = 0.003; less conserved regions: $\beta = 201.120$, SE= 70.017, t-value = 2.872, p-
466 value = 0.009).

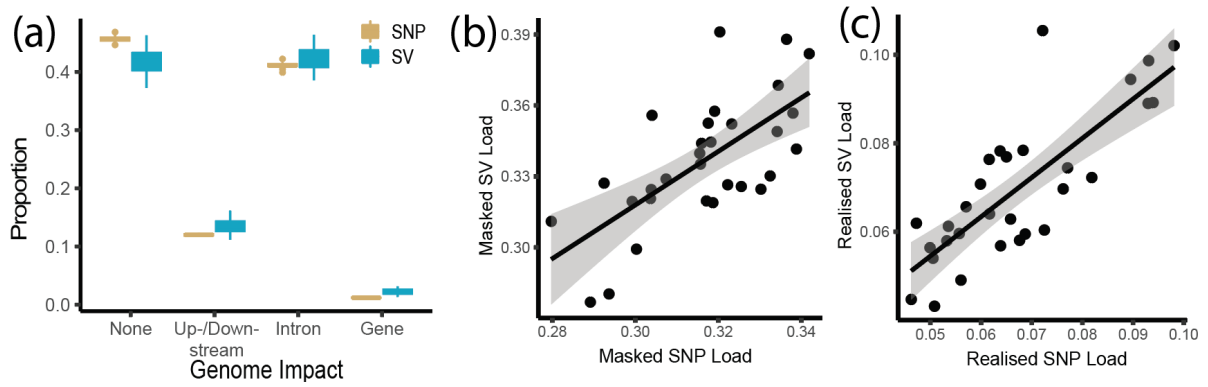
467



468

469 **Figure 1 | Genetic diversity and genomic distribution profiles of single nucleotide**
 470 **polymorphisms (SNPs) and structural variants (SVs) for hihi (*Notiomystis cincta*)**
 471 **individuals.** Panel (a) depicts the historic and present-day range of hihi on the North Island of
 472 Aotearoa New Zealand, with sampling locations from this study labelled with placenames. A
 473 depiction of the male and female hihi is also included (illustrations by Hui Zhen Tan). Panel (b)
 474 depicts the repeat annotations of the curated SVs. Panel (c) depicts the length profiles of the
 475 SVs pre- and post- transposable element (TE) filtering. The TE identity of the peaks in this plot
 476 are annotated with the primary TE responsible for the peak. Panel (d) is the site frequency
 477 spectrum of SNPs and SVs. Panel (e) is a boxplot of genotype frequencies across SNPs and SVs,
 478 averaged on a per-variant basis.

479



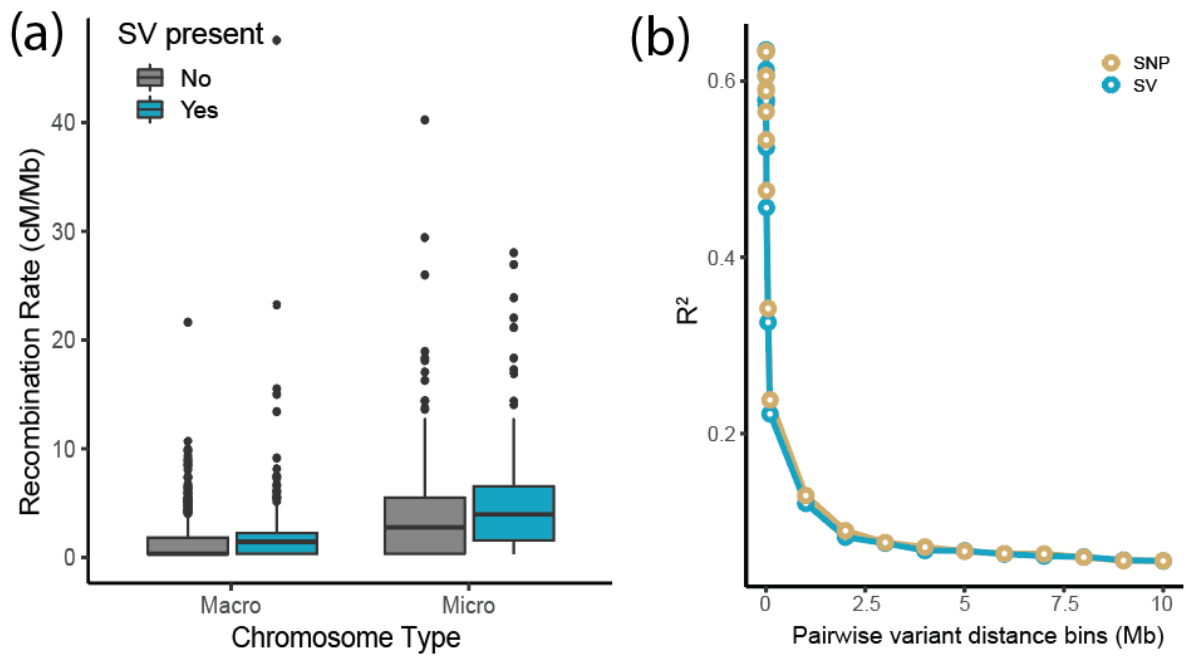
480

481 **Figure 2 | Patterns in variant impact and genetic load of single nucleotide polymorphisms**

482 **(SNPs) and structural variants (SVs).** Panel (a) is the proportion of SNP and SV minor allele
 483 variants within individuals that has been categorised based on their overlap with gene regions.

484 Panels (b) and (c) show the significant correlation between SV load and SNP load for masked
 485 and realised load respectively.

486

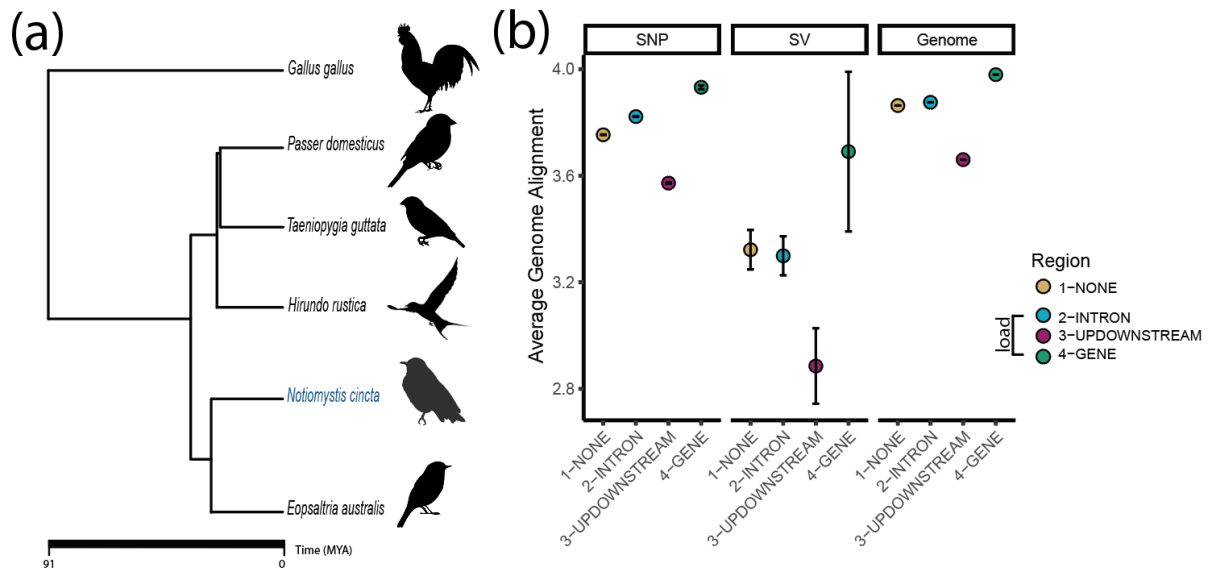


487

488 **Figure 3 | Structural variants in hihi in relation to recombination rates, linkage**

489 **disequilibrium, and minor allele frequency.** Panel (a) displays average recombination rate
 490 across 500Mb regions of the genome, classified by whether at least one SV is present with that
 491 region or not, and across either macro or micro chromosomes. Panel (b) displays linkage
 492 disequilibrium decay up to 10 Mb away from the SV variant breakends (or the SNP position).

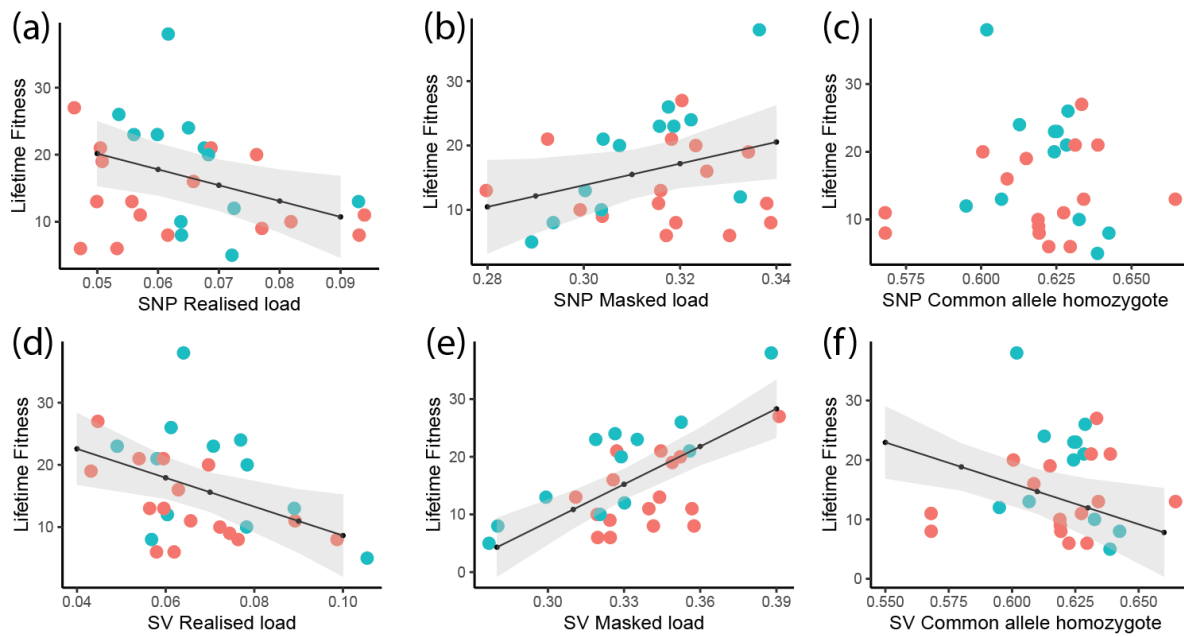
493



494

495 **Figure 4 | Evolutionary conservation and genome evolutionary conservation of the hihi**
 496 **across genomic locations of structural variant (SVs) and single nucleotide polymorphism**
 497 **(SNPs).** Panel (a) depicts the phylogenetic tree used in the PROGRESSIVE-CACTUS analysis, panel
 498 **(b)** depicts the average cross species conservation of genomic regions where different variant
 499 types and impact groups are located, where a value of 0 indicates a genomic sequence unique
 500 to the hihi, and a value of 5 indicates a region that is conserved across all species analysed.
 501 Pictures taken from <https://www.phylopic.org/>.

502



503

504 **Figure 5 | Impact of structural variant (SVs) and single nucleotide polymorphism (SNPs)**
 505 **realised load, masked load, and common allele homozygotes proportion on lifetime**
 506 **fitness of hihi on Tiritiri Matangi.** Scatterplot of the mutational load against the lifetime fitness,
 507 sex indicated by colour (female = red, male = blue), and mixed effect model fit lines indicated
 508 when the relationship with lifetime fitness was significant (or very near significance, in the case
 509 of SNP masked load). Two individuals from Te Hauturu-o-Toi were excluded from this analysis as
 510 no lifetime fitness values were available for them. Panel (a) shows SNP realised load, panel (b)
 511 shows SNP masked load, panel (c) shows SNP common allele homozygote proportion. Panel (d)
 512 shows SV realised load, panel (e) shows SV masked load, panel (f) shows SV common allele
 513 homozygote proportion.

514

515 **4 | Discussion**

516 Within small populations, conservation practitioners are particularly concerned with increased
517 inbreeding, loss of genetic diversity, and greater mutational load burdens (Dusseux et al., 2023).
518 In order to best track and manage these, the development of genomics-informed best practices
519 in conservation management requires that we understand how different components of the
520 genome contribute to functional genetic diversity. Through whole genome resequencing
521 approaches it is possible to quantify the more commonly studied single nucleotide
522 polymorphisms (SNPs) alongside structural variants (SVs), allowing us to achieve a more
523 holistic summary of inter-individual variation (Wellenreuther et al., 2019; Wold et al., 2021). In
524 this study, we specifically focus on load contributing genetic variation in SNPs and SVs and find
525 that masked and realised load is significantly but only moderately correlated across these two
526 genetic variant types. When testing for a relationship between load and lifetime fitness, there
527 was a significant negative relationship between realised load and fitness, and a significant
528 positive relationship between masked load and fitness for both SNPs and SVs. Interestingly,
529 when combining SNPs and SVs into the same model, SVs consistently had a stronger
530 correlation with fitness. However, of the four terms tested, only masked SV load remained
531 significantly correlated. This demonstrates that SVs are an important component of intra-
532 specific variation in the highly inbred and endangered hihi population on Tiritiri Matangi, and
533 that in order to optimise conservation genomic practice we may need to incorporate SV
534 profiling.

535 **4.1 | Mutational load may not be equivalent across SNPs and SVs in small populations**

536 Our results demonstrate that patterns of reduced genetic diversity in the hihi are just as evident
537 in SV as SNPs (Fig. S8) (Duntsch et al., 2021). Within the current study we have not identified
538 SVs as hidden source of unexpected genome wide patterns (Fig S7) or rare variants (Fig. 1d)
539 within the species, as has been found in some studies (Berdan et al., 2021; Stuart et al., 2023;
540 Weissensteiner et al., 2020). The observed moderate correlation between SNP and SV load
541 (44% for masked and 63% for realised load) indicates that within individuals, while one variant
542 type's load may be somewhat predicted by the other, SNPs do not act as a perfect proxy for SV
543 load (Fig. 2b & 2c). The moderate correlation could be explained by the differential
544 heterozygosity patterns between the marker types, with a slightly higher prevalence of
545 heterozygous SV than SNP genotypes in the population, alongside an enrichment of SVs in
546 regions of the genome with higher recombination rates (Fig. 1e, Fig. 3a). The deviation in
547 individual SNP and SV load contributes to differential patterns when linking individual load to

548 individual phenotype within the 28 assessed individuals. When testing both SNPs and SVs
549 concurrently, we identified only masked SV load as statistically correlated with lifetime fitness
550 within the successful hihi breeders used in this study (Fig. 5, Table S3) and found that this
551 pattern was apparent in both evolutionary conserved and unique genomic regions. Further,
552 though the joint SV and SNP realised load model was not significant, the magnitude of the
553 effects (β) suggests that SVs once again contributed more strongly to the negative correlation
554 with fitness than did SNPs (Table S3).

555 Genetic load in small, threatened populations is a result of the interaction between several
556 factors. Reduced efficacy of selection in small populations means that purifying selection is
557 less efficient because drift has a stronger effect (Brandvain & Wright, 2016; Dussex et al., 2023).
558 Drift also causes stochastic loss of genetic diversity (Jamieson et al., 2008), and loss of genetic
559 variants is further increased through elevated levels of inbreeding leading to effective purging of
560 highly deleterious variants (Dussex et al., 2021; Robinson et al., 2022). Although hihi were once
561 widespread across the North Island, it is likely that the remnant Te Hauturu-o-Toi island
562 population has historically been isolated and small (Duntsch et al., 2023). Impacts of human
563 settlement followed by a secondary extreme bottleneck of 21 individuals to found the Tiritiri
564 Matangi population in 1995-1996 (Armstrong et al., 2002; Duntsch et al., 2023) is likely to have
565 further impacted the landscape of genetic variation. Compounding on top of this is that
566 supplementary feeding supports a high population growth rate on Tiritiri Matangi, with the island
567 frequently used as a source of translocations (Ewen et al., 2013), which may also reduce the
568 strength of natural selection and encourage retention of mildly deleterious variants (Fronhofer
569 et al., 2024).

570 While this study only examined a small cohort of individuals the relationship between SV load
571 and hihi fitness supports the hypothesis that, while purging may have effectively removed the
572 most deleterious of variants, the strong effects of drift have led to mildly deleterious SVs
573 becoming more common in the Tiritiri Matangi population. This has been seen in another
574 recovered wild avian population, where highly deleterious variants were purged, but not
575 moderately deleterious ones (Femerling et al., 2023), and is also supported by signals of
576 genome-wide inbreeding depression in the population (Duntsch et al., 2023). Because SVs are
577 more likely to be deleterious than SNPs (Hämälä et al., 2021) and thus have likely faced stronger
578 purifying selection historically, this may mean that the weakened selection has resulted in a
579 relatively larger increase in SV based load than SNPs when considering patterns pre- and post-
580 the bottleneck imposed by reintroduction of hihi to Tiritiri Matangi. It is possible that more
581 deleterious variants exist within the hihi individuals that are not successful breeders. Future

582 work on this species will look to profile SVs across this species more broadly, to understand the
583 role they play in, for example, different life stages and how the SVs themselves are impacted by
584 demographic processes.

585 **4.2 | The relationship between mutational load and fitness**

586 In our results, we demonstrate that (when fitted alongside SNP load) there is only a significant
587 correlation between SV load and fitness when considering SV masked load, and not SV realised
588 load. Traditionally realised load is considered to be the load that is currently impacting
589 individuals, whereas it is both masked and realised that will impact future generations (Dussex
590 et al., 2023). However, this assumes the negative impact of load is conferred by recessive and
591 deleterious derived variants, whereas phenotypic expression could be impacted by other
592 effects such as additive or overdominance expression (Li et al., 2008), and it is possible that the
593 relationship between variant and phenotypic impact is stronger and/or more complex for SVs
594 than in SNPs (Buchanan & Scherer, 2008).

595 It is somewhat unexpected that SNP based load metrics were significantly (or borderline
596 significantly) correlated with fitness when tested individually, but were no longer so when tested
597 jointly with SV load. This may be because the SNP dataset captures roughly 3 million SNP
598 markers containing proportionally more neutral variation than the ~1,000 variants captured in
599 the SV dataset (Fig. 2a) (Collins et al., 2020; Hämälä et al., 2021). Even when reduced to the
600 ~54.7% of variants in proximity to genes during load calculations, it is likely that contributions of
601 realised and masked SNP load to fitness are made less apparent due to the predominance of
602 neutral markers, compared to the higher impact but lower density markers like SVs. When both
603 SNPs and SVs were fitted jointly, the stronger relationship between SV load and fitness also
604 suggests that much of the relationship between SNP load and fitness may have been driven by
605 linkage disequilibrium between (neutral) SNPs and nearby (mildly deleterious) SVs. Exploring
606 the application of additional approaches such as selection analysis (e.g. Gautier, 2015) to
607 further refine which components of genetic diversity are functional and contribute to load may
608 help to better capture functional variation for load calculations when working with high density
609 SNP makers generated from WGS data.

610 Ultimately, the results of this study demonstrate that identifying SVs allows us to capture unique
611 components of inter-individual genetic variation which may be vital for linking genetic patterns
612 to important phenotypic traits such as fitness, especially within this threatened species. Where
613 possible, WGS data should be equally interrogated for SNP and SV patterns, to understand the
614 distribution of more neutral SNPs and more deleterious SVs within the population. That being

615 said, mildly deleterious variants are important sources of functional genetic diversity that may
616 become beneficial under shifted selection engines, and ultimately any reduction of genetic
617 diversity reduces long-term adaptability to environmental shifts, i.e. adaptive potential
618 (Femerling et al., 2023; Kardos et al., 2021). Thus, to best manage populations with highly
619 reduced genetic diversity, the broad identification of genome wide variants is necessary, and
620 management processes that maximise heterozygosity may be most useful for future proofing
621 species of conservation concern.

622 **4.3 | SVs arise in regions of high recombination and low genome conservation**

623 The dynamic genomic recombination landscape that both causes and is impacted by SVs
624 (Mérot et al., 2020; Morgan et al., 2017) may explain the slightly steeper linkage disequilibrium
625 decay patterns seen in SVs compared to SNPs (Fig. 3b). The slightly weaker linkage
626 disequilibrium between SVs and surrounding SNPs may be due to biological reasons such as
627 recombination rate and differential selection impacts (Cumer et al., 2021; Pang et al., 2010), as
628 well as technical reasons caused by imperfect variant calling of both the SV and surrounding
629 SNPs (Audano & Beck, 2024; Geibel et al., 2022). The latter is likely to explain the highly
630 stochastic patterns seen in the immediate vicinity of the SV breakends (Fig. S10), while the
631 former may explain more distant pairwise patterns (Fig 3b).

632 We found that regions of high recombination are associated with the presence of SVs, and this
633 pattern is more evident on the micro-chromosomes within the hihi (Fig. 3a).

634 Microchromosomes are considered evolutionary building blocks in avians (Waters et al., 2021),
635 and our results indicate that these adaptive hotspots may encourage SVs which contribute to
636 adaptive diversity within a population (Fig. 3a). Higher levels of recombination on micro-
637 chromosomes can both cause novel variation and break up linkage disequilibrium between
638 variants, allowing adaptation to happen faster (Peischl et al., 2015) which in turn facilitates
639 more efficient evolution (Haenel et al., 2018). We see this trend in the evolutionary conservation
640 genome alignment results (Fig. 4) which demonstrate that SVs, regardless of their load
641 contribution, on average arise within more unique regions of the hihi genome. Intriguingly, within
642 micro-chromosomes load contributing SVs occur at higher frequencies than variants that do
643 not contribute to load, a pattern reversed in SNPs (Fig. S12). This may reflect genomic region
644 biases in which SVs and SNPs are likely to be created, as the former arise in high recombination
645 regions which are often the regions in which genes occur also (Tan et al., 2024).

646 **4.4 | Technical validation of SVs and exclusion of TEs**

647 Because of the size and complex nature of SVs, it is more technically challenging to identify
648 them in comparison to SNPs (Mahmoud et al., 2019; Wold et al., 2023). Through manual
649 curation of SVs the false positives may be reduced (Belyeu et al., 2018; Belyeu, Chowdhury, et
650 al., 2021), and the improvement in Mendelian inheritance errors in our data after manual
651 curation (Fig. S1-S6) is indicative that the process improved the accuracy of the SV dataset. We
652 also consider in our study the importance of excluding transposable element sequences from
653 analysis (Fig. 1b). Some of the aims of this study were to examine patterns of recombination and
654 evolutionary conservation near or at SVs and SNPs. TEs arise through self-replication and
655 relocation (Belyeu, Brand, et al., 2021; Biémont & Vieira, 2006), and so their relationship to
656 surrounding genomic features and patterns may interfere with identifying patterns pertinent to
657 non-TE SVs which themselves arise through mechanisms of DNA recombination, replication, or
658 repair (Carvalho & Lupski, 2016; Currall et al., 2013). It is also important to note that TE-
659 mediated SVs are more likely to introduce technical challenges during both SV identification
660 and genotyping in surrounding SNPs (Audano & Beck, 2024) and that targeted TE identification
661 processes (e.g. Chen et al., 2023) would be more appropriate for assessing TE specific load.

662 We found targeting breakends to be an efficient approach to removing the offending repeat
663 sequences from our final SV dataset (Fig. 1c), though note that profiling the impacts of TE load is
664 a pressing future direction in conservation biology, particularly in small threatened populations
665 that may experience greater stress and reduced TE suppression (Stapley et al., 2015).

666 **4.5 | Future directions**

667 The individuals used in this study were specifically successful breeders within the small Tiritiri
668 Matangi population, and so arguably may not carry the most deleterious variants. Despite this,
669 there was enough variation in slightly deleterious load across individuals, and enough variance
670 in fitness, to detect an impact of genetic load on lifetime fitness. Future directions of study in
671 this system will aim to profile SVs across a wider variety of individuals to identify correlations
672 between load and the presence or absence of successful breeding, as this may better capture a
673 wider range of deleterious homozygous minor alleles. We note also note that because of the
674 limits of profiling SVs with short reads (Mahmoud et al., 2019) our methods are not appropriate
675 for the detection of larger SVs. With the promise of increasingly affordable longer read
676 sequencing technologies we can begin to accurately characterise larger SVs (Schloissnig et al.,
677 2024) which are likely to have larger functional impacts which could impact fitness (Abel et al.,
678 2020).

679 Further, we note that our designation of the minor allele as the derived allele in assessing load
680 makes a number of the assumptions, namely that derived alleles are deleterious, that the
681 deleterious, derived allele will be the rarest, and that the rarest allele in our small dataset is the
682 minor allele in the population. Because hihi are phylogenetically distinct and even the closest
683 species do not have well-assembled genomes, it would be challenging to accurately polarise
684 even the SNP data. We also note that decreased evolutionary conservation for SVs relative to
685 SNPs (Fig. S12) means that outgroup selection will be more prone to bias with increasing
686 outgroup phylogenetic distance for the former variant type, indicating outgroup selection will be
687 very important for correct SV polarisation. As discussed above, the small population size is
688 likely to have led to some deleterious alleles reaching high frequencies by drift. Sampling a
689 small number of individuals from the population is also likely to have mis-identified the ‘correct’
690 realised load genotype. Indeed, the negative correlation between fitness and the major allele
691 homozygous genotype (Fig. 5c) may suggest that a number of realised load genotypes have
692 been incorrectly classified. We expect therefore that if variants can be successfully polarised,
693 the true realised load values will become be larger and the relationship with fitness stronger
694 (Keightley & Jackson, 2018).

695 Finally, restricting load calculations to gene-proximate regions ignores the functional role non-
696 coding regions of the genome may play in influencing phenotype. Sequence variation can
697 influence phenotype through, for example, alterations to cis -regulatory elements and three
698 dimensional structure DNA (Engreitz et al., 2016; Soto et al., 2023; Spielmann & Mundlos,
699 2016), which will undoubtedly be differentially impacted by SNP and in particular SV variants.
700 Thus, limiting load estimates to coding regions of the genome may neglect important functional
701 variation within a population, impacting our ability to accurately identify and predict the
702 adaptive potential for a species (Kardos et al., 2021), and is another avenue for future research
703 within this system and also more broadly within conservation genomics.

704 **5 | Conclusion**

705 In highly inbred species like the hihi, identifying all aspects of functional genetic diversity is
706 extremely important. Previous research in the hihi has found fairly low adaptive potential as
707 interpreted from low heritability of fitness and fitness-associated traits (de Villemereuil et al.,
708 2019). However, quantifying a more comprehensive genome-wide profile of intra-individual
709 variation has revealed previously hidden associations between fitness and underlying genetic
710 variant patterns. This study demonstrates that the SV variants contain important aspects of
711 variation that may be highly applicable to conservation decisions within a species. This study

712 joins the many that demonstrate the non-redundant genomic variation captured by structural
713 variants may have important functional implications (e.g. Catanach et al., 2019; Li et al., 2024;
714 Rafter et al., 2021), and reveals that our ability to assess genetic diversity and load in small
715 populations will always be limited if we only investigate SNPs.

716

717 **Author contributions**

718 Project conceived by AWS and KCS. Sample coordination and extractions performed by SP.
719 Analysis and manuscript drafting was completed by KCS, with additional data from HZT and AW.
720 Additional resources were supplied by PB and JGE. All authors edited and contributed to the
721 final version of this manuscript.

722 **Data availability**

723 Hihi are of cultural significance to the Indigenous People of Aotearoa New Zealand, the Māori
724 and are considered a taonga (treasured) species whose whakapapa (genealogy) is intricately
725 tied to that of Māori. The sequencing and variant data generated as part of this study will be
726 made available on request though the recommendation of Ngāti Manuhiri, the iwi (extended
727 kinship group) that affiliates as kaitiaki (guardians) for hihi. To obtain contact details for the iwi,
728 please contact Dr Anna Santure: a.santure@auckland.ac.nz. All of the code associated with
729 this project will be made available through GitHub at
730 (https://github.com/katarinastuart/Nc3_HihiSV).

731 **Acknowledgements**

732 We acknowledge Ngāti Manuhiri as Mana Whenua and Kaitiaki of Te Hauturu-o-Toi and its
733 taonga, including hihi. We extend many thanks to the volunteers, past students and Department
734 of Conservation staff who have contributed to monitoring the Tiritiri Mātangi hihi population. We
735 thank the Hihi Recovery Group, Department of Conservation, and Supporters of Tiritiri Mātangi
736 for maintaining such a long-term vision in monitoring and management of this population, with
737 a special mention of the current hihi conservation officer Mhairi McCready. We acknowledge
738 the use of New Zealand eScience Infrastructure (NeSI) high-performance computing facilities,
739 and thank the NeSI team, particularly Dinindu Senanayake, for all their support. We also thank
740 the AgResearch Animal Genomics team, particularly Tracey Van Stijn, Rudiger Brauning and
741 Shannon Clarke, for hihi Illumina sequencing. Many thanks to Jana Wold and Joseph Guhlin for
742 helpful feedback and discussion on SVs and whole genome alignment. Open access publishing
743 facilitated by The University of Auckland, as organised by the Council of Australian University

744 Librarians and its Member Institutions. All work was undertaken in accordance with Department
745 of Conservation permits 53614-FAU and 66751-FAU. The High Quality Genomes, and High
746 Quality Genomes and Population Genomics (HQG+PG) projects I and II of Genomics Aotearoa
747 supported AWS, AW and KS and funded the whole genome resequencing data and sequencing
748 of the reference genome utilised in this study. Funding from the George Mason Center for the
749 Natural Environment and the Little Barrier Island (Hauturu) Supporters Trust supported
750 fieldwork collection from Te Hauturu-o-Toi. A Marsden Grant (UOA1408) awarded to AWS from
751 the New Zealand Royal Society Te Aparangi supported AWS, PB, and JGE and funded
752 development of the SNP array genotypes and microsatellite genotyping. A Strategic Science
753 Investment Fund in Data Science from the Ministry of Business, Innovation and Employment
754 supports AWS and HZT. PB and JGE are supported by Research England.

755

756 **REFERENCES:**

- 757 Abel, H. J., Larson, D. E., Regier, A. A., Chiang, C., Das, I., Kanchi, K. L., Layer, R. M., Neale, B.
758 M., Salerno, W. J., Reeves, C., Buyske, S., Matise, T. C., Muzny, D. M., Zody, M. C., Lander,
759 E. S., Dutcher, S. K., Stitzel, N. O., & Hall, I. M. (2020). Mapping and characterization of
760 structural variation in 17,795 human genomes. *Nature*, *583*(7814), 83–89.
761 <https://doi.org/10.1038/s41586-020-2371-0>
- 762 Alves, F., Banks, S. C., Edworthy, M., Stojanovic, D., Langmore, N. E., & Heinsohn, R. (2023).
763 Using conservation genetics to prioritise management options for an endangered
764 songbird. *Heredity*, *130*(5), 289–301. <https://doi.org/10.1038/s41437-023-00609-6>
- 765 Armstrong, D. P., Davidson, R. S., Dimond, W. J., Perrott, J. K., Castro, I., Ewen, J. G., Griffiths, R.,
766 & Taylor, J. (2002). Population dynamics of reintroduced forest birds on New Zealand
767 islands. *Journal of Biogeography*, *29*(5–6), 609–621. [https://doi.org/10.1046/j.1365-](https://doi.org/10.1046/j.1365-2699.2002.00710.x)
768 [2699.2002.00710.x](https://doi.org/10.1046/j.1365-2699.2002.00710.x)
- 769 Armstrong, J., Hickey, G., Diekhans, M., Fiddes, I. T., Novak, A. M., Deran, A., Fang, Q., Xie, D.,
770 Feng, S., Stiller, J., Genreux, D., Johnson, J., Marinescu, V. D., Alföldi, J., Harris, R. S.,
771 Lindblad-Toh, K., Haussler, D., Karlsson, E., Jarvis, E. D., ... Paten, B. (2020). Progressive
772 Cactus is a multiple-genome aligner for the thousand-genome era. *Nature*, *587*(7833),
773 246–251. <https://doi.org/10.1038/s41586-020-2871-y>
- 774 Audano, P. A., & Beck, C. R. (2024). Small polymorphisms are a source of ancestral bias in
775 structural variant breakpoint placement. *Genome Research*, *34*(1), 7–19.
776 <https://doi.org/10.1101/gr.278203.123>
- 777 Bailey, S., Guhlin, J., Senanayake, D. S., Scherer, P., Brekke, P., Ewen, J. G., Santure, A. W., &
778 Whibley, A. (2023). Assembly of female and male hihi genomes (stitchbird; *Notiomystis*
779 *cincta*) enables characterization of the W chromosome and resources for conservation
780 genomics. *Molecular Ecology Resources*, *n/a*(*n/a*). [https://doi.org/10.1111/1755-](https://doi.org/10.1111/1755-0998.13823)
781 [0998.13823](https://doi.org/10.1111/1755-0998.13823)

782 Bates, D., Mächler, M., Bolker, B., & Walker, S. (2015). Fitting Linear Mixed-Effects Models Using
783 lme4. *Journal of Statistical Software*, 67(1), Article 1.
784 <https://doi.org/10.18637/jss.v067.i01>

785 Belyeu, J. R., Brand, H., Wang, H., Zhao, X., Pedersen, B. S., Feusier, J., Gupta, M., Nicholas, T. J.,
786 Brown, J., Baird, L., Devlin, B., Sanders, S. J., Jorde, L. B., Talkowski, M. E., & Quinlan, A.
787 R. (2021). De novo structural mutation rates and gamete-of-origin biases revealed
788 through genome sequencing of 2,396 families. *American Journal of Human Genetics*,
789 108(4), 597–607. <https://doi.org/10.1016/j.ajhg.2021.02.012>

790 Belyeu, J. R., Chowdhury, M., Brown, J., Pedersen, B. S., Cormier, M. J., Quinlan, A. R., & Layer, R.
791 M. (2021). Samplot: A platform for structural variant visual validation and automated
792 filtering. *Genome Biology*, 22(1), 161. <https://doi.org/10.1186/s13059-021-02380-5>

793 Belyeu, J. R., Nicholas, T. J., Pedersen, B. S., Sasani, T. A., Havrilla, J. M., Kravitz, S. N., Conway,
794 M. E., Lohman, B. K., Quinlan, A. R., & Layer, R. M. (2018). SV-plaudit: A cloud-based
795 framework for manually curating thousands of structural variants. *GigaScience*, 7(7),
796 giy064. <https://doi.org/10.1093/gigascience/giy064>

797 Berdan, E. L., Mérot, C., Pavia, H., Johannesson, K., Wellenreuther, M., & Butlin, R. K. (2021). A
798 large chromosomal inversion shapes gene expression in seaweed flies (*Coelopa frigida*).
799 *Evolution Letters*, 5(6), 607–624. <https://doi.org/10.1002/evl3.260>

800 Biémont, C., & Vieira, C. (2006). Junk DNA as an evolutionary force. *Nature*, 443(7111), Article
801 7111. <https://doi.org/10.1038/443521a>

802 Brandvain, Y., & Wright, S. I. (2016). The Limits of Natural Selection in a Nonequilibrium World.
803 *Trends in Genetics*, 32(4), 201–210. <https://doi.org/10.1016/j.tig.2016.01.004>

804 Brekke, P., Bennett, P. M., Santure, A. W., & Ewen, J. G. (2011). High genetic diversity in the
805 remnant island population of hihi and the genetic consequences of re-introduction.
806 *Molecular Ecology*, 20(1), 29–45. <https://doi.org/10.1111/j.1365-294X.2010.04923.x>

807 Brekke, P., Dawson, D. A., Horsburgh, G. J., & Ewen, J. G. (2009). Characterization of
808 microsatellite loci in the hihi *Notiomystis cincta* (Notiomystidae, Aves). *Molecular*
809 *Ecology Resources*, 9(4), 1255–1258. <https://doi.org/10.1111/j.1755-0998.2009.02626.x>

810 Buchanan, J. A., & Scherer, S. W. (2008). Contemplating effects of genomic structural variation.
811 *Genetics in Medicine*, 10(9), 639–647. <https://doi.org/10.1097/GIM.0b013e318183f848>

812 Cao, J., Schneeberger, K., Ossowski, S., Günther, T., Bender, S., Fitz, J., Koenig, D., Lanz, C.,
813 Stegle, O., Lippert, C., Wang, X., Ott, F., Müller, J., Alonso-Blanco, C., Borgwardt, K.,
814 Schmid, K. J., & Weigel, D. (2011). Whole-genome sequencing of multiple *Arabidopsis*
815 *thaliana* populations. *Nature Genetics*, 43(10), 956–963. <https://doi.org/10.1038/ng.911>

816 Carvalho, C. M. B., & Lupski, J. R. (2016). Mechanisms underlying structural variant formation in
817 genomic disorders. *Nature Reviews. Genetics*, 17(4), 224–238.
818 <https://doi.org/10.1038/nrg.2015.25>

819 Catanach, A., Crowhurst, R., Deng, C., David, C., Bernatchez, L., & Wellenreuther, M. (2019).
820 The genomic pool of standing structural variation outnumbers single nucleotide
821 polymorphism by threefold in the marine teleost *Chrysophrys auratus*. *Molecular*
822 *Ecology*, 28(6), 1210–1223. <https://doi.org/10.1111/mec.15051>

823 Chakraborty, M., Emerson, J. J., Macdonald, S. J., & Long, A. D. (2019). Structural variants exhibit
824 widespread allelic heterogeneity and shape variation in complex traits. *Nature*
825 *Communications*, 10(1), 4872. <https://doi.org/10.1038/s41467-019-12884-1>

826 Chen, J., Basting, P. J., Han, S., Garfinkel, D. J., & Bergman, C. M. (2023). Reproducible
827 evaluation of transposable element detectors with McClintock 2 guides accurate
828 inference of Ty insertion patterns in yeast. *Mobile DNA*, 14(1), 8.
829 <https://doi.org/10.1186/s13100-023-00296-4>

830 Chen, X., Schulz-Trieglaff, O., Shaw, R., Barnes, B., Schlesinger, F., Källberg, M., Cox, A. J.,
831 Kruglyak, S., & Saunders, C. T. (2016). Manta: Rapid detection of structural variants and

832 indels for germline and cancer sequencing applications. *Bioinformatics (Oxford,*
833 *England)*, 32(8), 1220–1222. <https://doi.org/10.1093/bioinformatics/btv710>

834 Collins, R. L., Brand, H., Karczewski, K. J., Zhao, X., Alföldi, J., Francioli, L. C., Khera, A. V.,
835 Lowther, C., Gauthier, L. D., Wang, H., Watts, N. A., Solomonson, M., O'Donnell-Luria,
836 A., Baumann, A., Munshi, R., Walker, M., Whelan, C. W., Huang, Y., Brookings, T., ...
837 Talkowski, M. E. (2020). A structural variation reference for medical and population
838 genetics. *Nature*, 581(7809), 444–451. <https://doi.org/10.1038/s41586-020-2287-8>

839 Cumer, T., Boyer, F., & Pompanon, F. (2021). Genome-Wide Detection of Structural Variations
840 Reveals New Regions Associated with Domestication in Small Ruminants. *Genome*
841 *Biology and Evolution*, 13(8), evab165. <https://doi.org/10.1093/gbe/evab165>

842 Currall, B. B., Chiang, C., Talkowski, M. E., & Morton, C. C. (2013). Mechanisms for Structural
843 Variation in the Human Genome. *Current Genetic Medicine Reports*, 1(2), 81–90.
844 <https://doi.org/10.1007/s40142-013-0012-8>

845 Danecek, P., Auton, A., Abecasis, G., Albers, C. A., Banks, E., DePristo, M. A., Handsaker, R. E.,
846 Lunter, G., Marth, G. T., Sherry, S. T., McVean, G., & Durbin, R. (2011). The variant call
847 format and VCFtools. *Bioinformatics*, 27(15), 2156–2158.
848 <https://doi.org/10.1093/bioinformatics/btr330>

849 Danecek, P., Bonfield, J. K., Liddle, J., Marshall, J., Ohan, V., Pollard, M. O., Whitwham, A.,
850 Keane, T., McCarthy, S. A., Davies, R. M., & Li, H. (2021). Twelve years of SAMtools and
851 BCFtools. *GigaScience*, 10(2), giab008. <https://doi.org/10.1093/gigascience/giab008>

852 de Villemereuil, P., Rutschmann, A., Lee, K. D., Ewen, J. G., Brekke, P., & Santure, A. W. (2019).
853 Little Adaptive Potential in a Threatened Passerine Bird. *Current Biology*, 29(5), 889-
854 894.e3. <https://doi.org/10.1016/j.cub.2019.01.072>

855 Doerr, L. R., Richardson, K. M., Ewen, J. G., & Armstrong, D. P. (2017). Effect of supplementary
856 feeding on reproductive success of hihi (stitchbird, *Notiomystis cincta*) at a mature

857 forest reintroduction site. *New Zealand Journal of Ecology*, 41(1), Article 1.
858 <https://doi.org/10.20417/nzjecol.41.15>

859 Duckett, D. J., Calder, K., Sullivan, J., Tank, D. C., & Carstens, B. C. (2023). Reduced
860 representation approaches produce similar results to whole genome sequencing for
861 some common phylogeographic analyses. *PLOS ONE*, 18(11), e0291941.
862 <https://doi.org/10.1371/journal.pone.0291941>

863 Duntsch, L., Whibley, A., Brekke, P., Ewen, J. G., & Santure, A. W. (2021). Genomic data of
864 different resolutions reveal consistent inbreeding estimates but contrasting
865 homozygosity landscapes for the threatened Aotearoa New Zealand hihi. *Molecular
866 Ecology*, 30(23), 6006–6020. <https://doi.org/10.1111/mec.16068>

867 Duntsch, L., Whibley, A., de Villemereuil, P., Brekke, P., Bailey, S., Ewen, J. G., & Santure, A. W.
868 (2023). Genomic signatures of inbreeding depression for a threatened Aotearoa New
869 Zealand passerine. *Molecular Ecology*, 32(8), 1893–1907.
870 <https://doi.org/10.1111/mec.16855>

871 Dussex, N., Morales, H. E., Grossen, C., Dalén, L., & Oosterhout, C. van. (2023). Purging and
872 accumulation of genetic load in conservation. *Trends in Ecology & Evolution*, 38(10),
873 961–969. <https://doi.org/10.1016/j.tree.2023.05.008>

874 Dussex, N., van der Valk, T., Morales, H. E., Wheat, C. W., Díez-del-Molino, D., von Seth, J.,
875 Foster, Y., Kutschera, V. E., Guschanski, K., Rhie, A., Phillippy, A. M., Korlach, J., Howe,
876 K., Chow, W., Pelan, S., Mendes Damas, J. D., Lewin, H. A., Hastie, A. R., Formenti, G., ...
877 Dalén, L. (2021). Population genomics of the critically endangered kākāpō. *Cell
878 Genomics*, 1(1), 100002. <https://doi.org/10.1016/j.xgen.2021.100002>

879 Edmonds, C. A., Lillie, A. S., & Cavalli-Sforza, L. L. (2004). Mutations arising in the wave front of
880 an expanding population. *Proceedings of the National Academy of Sciences*, 101(4),
881 975–979. <https://doi.org/10.1073/pnas.0308064100>

882 Engreitz, J. M., Ollikainen, N., & Guttman, M. (2016). Long non-coding RNAs: Spatial amplifiers
883 that control nuclear structure and gene expression. *Nature Reviews Molecular Cell*
884 *Biology*, 17(12), 756–770. <https://doi.org/10.1038/nrm.2016.126>

885 Ewels, P., Magnusson, M., Lundin, S., & Käller, M. (2016). MultiQC: Summarize analysis results
886 for multiple tools and samples in a single report. *Bioinformatics*, 32(19), 3047–3048.
887 <https://doi.org/10.1093/bioinformatics/btw354>

888 Ewen, J. G., Renwick, R., Adams, L., Armstrong, D. P., Parker, K. A., & North, N. Z. D. (2013).
889 1980-2012: 32 years of re-introduction efforts of the hihi (stitchbird) in New Zealand.
890 *Global Re-Introduction Perspectives: 2013. Further Case Studies from around the*
891 *Globe*, 68.
892 https://www.academia.edu/download/43117316/rsg_book_2013.pdf#page=83

893 Femerling, G., van Oosterhout, C., Feng, S., Bristol, R. M., Zhang, G., Groombridge, J., P. Gilbert,
894 M. T., & Morales, H. E. (2023). Genetic Load and Adaptive Potential of a Recovered Avian
895 Species that Narrowly Avoided Extinction. *Molecular Biology and Evolution*, 40(12),
896 msad256. <https://doi.org/10.1093/molbev/msad256>

897 Frankham, R. (2008). Genetic adaptation to captivity in species conservation programs.
898 *Molecular Ecology*, 17(1), 325–333. <https://doi.org/10.1111/j.1365-294X.2007.03399.x>

899 Fronhofer, E. A., Govaert, L., O'Connor, M. I., Schreiber, S. J., & Altermatt, F. (2024). The shape of
900 density dependence and the relationship between population growth, intraspecific
901 competition and equilibrium population density. *Oikos*, 2024(2), e09824.
902 <https://doi.org/10.1111/oik.09824>

903 Fuentes-Pardo, A. P., & Ruzzante, D. E. (2017). Whole-genome sequencing approaches for
904 conservation biology: Advantages, limitations and practical recommendations.
905 *Molecular Ecology*, 26(20), 5369–5406. <https://doi.org/10.1111/mec.14264>

906 Gautier, M. (2015). Genome-Wide Scan for Adaptive Divergence and Association with
907 Population-Specific Covariates. *Genetics*, 201(4), 1555–1579.
908 <https://doi.org/10.1534/genetics.115.181453>

909 Geibel, J., Praefke, N. P., Weigend, S., Simianer, H., & Reimer, C. (2022). Assessment of linkage
910 disequilibrium patterns between structural variants and single nucleotide
911 polymorphisms in three commercial chicken populations. *BMC Genomics*, 23, 193.
912 <https://doi.org/10.1186/s12864-022-08418-7>

913 Haenel, Q., Laurentino, T. G., Roesti, M., & Berner, D. (2018). Meta-analysis of chromosome-
914 scale crossover rate variation in eukaryotes and its significance to evolutionary
915 genomics. *Molecular Ecology*, 27(11), 2477–2497. <https://doi.org/10.1111/mec.14699>

916 Haig, S. M., Miller, Mark. P., Bellinger, R., Draheim, H. M., Mercer, D. M., & Mullins, T. D. (2016).
917 The conservation genetics juggling act: Integrating genetics and ecology, science and
918 policy. *Evolutionary Applications*, 9(1), 181–195. <https://doi.org/10.1111/eva.12337>

919 Hämälä, T., Wafula, E. K., Guiltinan, M. J., Ralph, P. E., dePamphilis, C. W., & Tiffin, P. (2021).
920 Genomic structural variants constrain and facilitate adaptation in natural populations of
921 *Theobroma cacao*, the chocolate tree. *Proceedings of the National Academy of
922 Sciences*, 118(35). <https://doi.org/10.1073/pnas.2102914118>

923 Hedrick, P. W., Hellsten, U., & Grattapaglia, D. (2016). Examining the cause of high inbreeding
924 depression: Analysis of whole-genome sequence data in 28 selfed progeny of
925 *Eucalyptus grandis*. *New Phytologist*, 209(2), 600–611.
926 <https://doi.org/10.1111/nph.13639>

927 Hickey, G., Paten, B., Earl, D., Zerbino, D., & Haussler, D. (2013). HAL: A hierarchical format for
928 storing and analyzing multiple genome alignments. *Bioinformatics*, 29(10), 1341–1342.
929 <https://doi.org/10.1093/bioinformatics/btt128>

930 Hohenlohe, P. A., Funk, W. C., & Rajora, O. P. (2021). Population genomics for wildlife
931 conservation and management. *Molecular Ecology*, 30(1), 62–82.
932 <https://doi.org/10.1111/mec.15720>

933 Humble, E., Stoffel, M. A., Dicks, K., Ball, A. D., Gooley, R. M., Chuyen, J., Pusey, R., Remeithi, M.
934 A., Koepfli, K.-P., Pukazhenthii, B., Senn, H., & Ogden, R. (2023). Conservation
935 management strategy impacts inbreeding and mutation load in scimitar-horned oryx.
936 *Proceedings of the National Academy of Sciences*, 120(18), e2210756120.
937 <https://doi.org/10.1073/pnas.2210756120>

938 Jamieson, I. G., Grueber, C. E., Waters, J. M., & Gleeson, D. M. (2008). Managing genetic diversity
939 in threatened populations: A New Zealand perspective. *New Zealand Journal of Ecology*,
940 32(1), 130–137. <https://www.jstor.org/stable/24058111>

941 Jeffares, D. C., Jolly, C., Hoti, M., Speed, D., Shaw, L., Rallis, C., Balloux, F., Dessimoz, C., Bähler,
942 J., & Sedlazeck, F. J. (2017). Transient structural variations have strong effects on
943 quantitative traits and reproductive isolation in fission yeast. *Nature Communications*,
944 8(1), 14061. <https://doi.org/10.1038/ncomms14061>

945 Kardos, M., Armstrong, E. E., Fitzpatrick, S. W., Hauser, S., Hedrick, P. W., Miller, J. M., Tallmon,
946 D. A., & Funk, W. C. (2021). The crucial role of genome-wide genetic variation in
947 conservation. *Proceedings of the National Academy of Sciences*, 118(48),
948 e2104642118. <https://doi.org/10.1073/pnas.2104642118>

949 Keightley, P. D., & Jackson, B. C. (2018). Inferring the Probability of the Derived vs. The Ancestral
950 Allelic State at a Polymorphic Site. *Genetics*, 209(3), 897–906.
951 <https://doi.org/10.1534/genetics.118.301120>

952 Kreiner, J. M., Giacomini, D. A., Bemm, F., Waithaka, B., Regalado, J., Lanz, C., Hildebrandt, J.,
953 Sikkema, P. H., Tranel, P. J., Weigel, D., Stinchcombe, J. R., & Wright, S. I. (2019). Multiple
954 modes of convergent adaptation in the spread of glyphosate-resistant *Amaranthus*

955 tuberculatus. *Proceedings of the National Academy of Sciences*, 116(42), 21076–21084.
956 <https://doi.org/10.1073/pnas.1900870116>

957 Krueger, F. (2021). *Babraham Bioinformatics—Trim Galore!* (0.6.7) [Computer software].
958 https://www.bioinformatics.babraham.ac.uk/projects/trim_galore/

959 Kumar, S., Suleski, M., Craig, J. M., Kasprowicz, A. E., Sanderford, M., Li, M., Stecher, G., &
960 Hedges, S. B. (2022). TimeTree 5: An Expanded Resource for Species Divergence Times.
961 *Molecular Biology and Evolution*, 39(8), msac174.
962 <https://doi.org/10.1093/molbev/msac174>

963 Layer, R. M., Chiang, C., Quinlan, A. R., & Hall, I. M. (2014). LUMPY: A probabilistic framework for
964 structural variant discovery. *Genome Biology*, 15(6), R84. [https://doi.org/10.1186/gb-](https://doi.org/10.1186/gb-2014-15-6-r84)
965 2014-15-6-r84

966 Li, H. (2013). Aligning sequence reads, clone sequences and assembly contigs with BWA-MEM.
967 *arXiv:1303.3997 [q-Bio]*. <http://arxiv.org/abs/1303.3997>

968 Li, H., Handsaker, B., Wysoker, A., Fennell, T., Ruan, J., Homer, N., Marth, G., Abecasis, G.,
969 Durbin, R., & 1000 Genome Project Data Processing Subgroup. (2009). The Sequence
970 Alignment/Map format and SAMtools. *Bioinformatics (Oxford, England)*, 25(16), 2078–
971 2079. <https://doi.org/10.1093/bioinformatics/btp352>

972 Li, L., Lu, K., Chen, Z., Mu, T., Hu, Z., & Li, X. (2008). Dominance, Overdominance and Epistasis
973 Condition the Heterosis in Two Heterotic Rice Hybrids. *Genetics*, 180(3), 1725–1742.
974 <https://doi.org/10.1534/genetics.108.091942>

975 Li, Y., Yao, J., Sang, H., Wang, Q., Su, L., Zhao, X., Xia, Z., Wang, F., Wang, K., Lou, D., Wang, G.,
976 Waterhouse, R. M., Wang, H., Luo, S., & Sun, C. (2024). Pan-genome analysis highlights
977 the role of structural variation in the evolution and environmental adaptation of Asian
978 honeybees. *Molecular Ecology Resources*, 24(2), e13905. [https://doi.org/10.1111/1755-](https://doi.org/10.1111/1755-0998.13905)
979 0998.13905

980 Lohmueller, K. E. (2014). The Impact of Population Demography and Selection on the Genetic
981 Architecture of Complex Traits. *PLoS Genetics*, 10(5), e1004379.
982 <https://doi.org/10.1371/journal.pgen.1004379>

983 Lynch, M., & O’Hely, M. (2001). Captive breeding and the genetic fitness of natural populations.
984 *Conservation Genetics*, 2(4), 363–378. <https://doi.org/10.1023/A:1012550620717>

985 Mahmoud, M., Gobet, N., Cruz-Dávalos, D. I., Mounier, N., Dessimoz, C., & Sedlazeck, F. J.
986 (2019). Structural variant calling: The long and the short of it. *Genome Biology*, 20(1),
987 246. <https://doi.org/10.1186/s13059-019-1828-7>

988 McLaren, W., Gil, L., Hunt, S. E., Riat, H. S., Ritchie, G. R. S., Thormann, A., Flicek, P., &
989 Cunningham, F. (2016). The Ensembl Variant Effect Predictor. *Genome Biology*, 17(1),
990 122. <https://doi.org/10.1186/s13059-016-0974-4>

991 McMahon, B. J., Teeling, E. C., & Höglund, J. (2014). How and why should we implement
992 genomics into conservation? *Evolutionary Applications*, 7(9), 999–1007.
993 <https://doi.org/10.1111/eva.12193>

994 Mérot, C., Oomen, R. A., Tigano, A., & Wellenreuther, M. (2020). A Roadmap for Understanding
995 the Evolutionary Significance of Structural Genomic Variation. *Trends in Ecology &*
996 *Evolution*, 35(7), 561–572. <https://doi.org/10.1016/j.tree.2020.03.002>

997 Miskelly, C. M., & Powlesland, R. G. (2013). Conservation translocations of New Zealand birds
998 1863-2012. *Notornis*, 60, 3–28.

999 Morgan, A. P., Gatti, D. M., Najarian, M. L., Keane, T. M., Galante, R. J., Pack, A. I., Mott, R.,
1000 Churchill, G. A., & de Villena, F. P.-M. (2017). Structural Variation Shapes the Landscape
1001 of Recombination in Mouse. *Genetics*, 206(2), 603–619.
1002 <https://doi.org/10.1534/genetics.116.197988>

1003 Nichols, S., Ewen, J. G., Gottelli, D., Grueber, C. E., Santure, A. W., Trask, A., & Brekke, P. (2024).
1004 Genetic rescue attempt in a small, inbred population of a wild endangered passerine.
1005 *Biological Conservation*, 290, 110430. <https://doi.org/10.1016/j.biocon.2023.110430>

1006 Pang, A. W., MacDonald, J. R., Pinto, D., Wei, J., Rafiq, M. A., Conrad, D. F., Park, H., Hurles, M.
1007 E., Lee, C., Venter, J. C., Kirkness, E. F., Levy, S., Feuk, L., & Scherer, S. W. (2010).
1008 Towards a comprehensive structural variation map of an individual human genome.
1009 *Genome Biology*, 11(5), R52. <https://doi.org/10.1186/gb-2010-11-5-r52>

1010 Parlato, E. H., Ewen, J. G., McCreedy, M., Parker, K. A., & Armstrong, D. P. (2021). A modelling
1011 framework for integrating reproduction, survival and count data when projecting the
1012 fates of threatened populations. *Oecologia*, 195(3), 627–640.
1013 <https://doi.org/10.1007/s00442-021-04871-5>

1014 Peischl, S., Kirkpatrick, M., & Excoffier, L. (2015). Expansion Load and the Evolutionary
1015 Dynamics of a Species Range. *The American Naturalist*, 185(4), E81–E93.
1016 <https://doi.org/10.1086/680220>

1017 *Picard toolkit*. (2019). [Computer software]. Broad Institute.
1018 <http://broadinstitute.github.io/picard/>

1019 Purcell, S., Neale, B., Todd-Brown, K., Thomas, L., Ferreira, M. A. R., Bender, D., Maller, J., Sklar,
1020 P., de Bakker, P. I. W., Daly, M. J., & Sham, P. C. (2007). PLINK: A Tool Set for Whole-
1021 Genome Association and Population-Based Linkage Analyses. *American Journal of*
1022 *Human Genetics*, 81(3), 559–575.
1023 <https://www.ncbi.nlm.nih.gov/pmc/articles/PMC1950838/>

1024 Rafter, P., Gormley, I. C., Parnell, A. C., Naderi, S., & Berry, D. P. (2021). The Contribution of Copy
1025 Number Variants and Single Nucleotide Polymorphisms to the Additive Genetic
1026 Variance of Carcass Traits in Cattle. *Frontiers in Genetics*, 12, 761503.
1027 <https://doi.org/10.3389/fgene.2021.761503>

1028 Rausch, T., Zichner, T., Schlattl, A., Stütz, A. M., Benes, V., & Korbel, J. O. (2012). DELLY:
1029 Structural variant discovery by integrated paired-end and split-read analysis.
1030 *Bioinformatics (Oxford, England)*, 28(18), i333–i339.
1031 <https://doi.org/10.1093/bioinformatics/bts378>

1032 Robinson, J. A., Kyriazis, C. C., Nigenda-Morales, S. F., Beichman, A. C., Rojas-Bracho, L.,
1033 Robertson, K. M., Fontaine, M. C., Wayne, R. K., Lohmueller, K. E., Taylor, B. L., & Morin,
1034 P. A. (2022). The critically endangered vaquita is not doomed to extinction by inbreeding
1035 depression. *Science*, 376(6593), 635–639. <https://doi.org/10.1126/science.abm1742>
1036 Ruigrok, M., Xue, B., Catanach, A., Zhang, M., Jesson, L., Davy, M., & Wellenreuther, M. (2022).
1037 The Relative Power of Structural Genomic Variation versus SNPs in Explaining the
1038 Quantitative Trait Growth in the Marine Teleost *Chrysophrys auratus*. *Genes*, 13(7),
1039 1129. <https://doi.org/10.3390/genes13071129>
1040 Scherer, S. W., Lee, C., Birney, E., Altshuler, D. M., Eichler, E. E., Carter, N. P., Hurles, M. E., &
1041 Feuk, L. (2007). Challenges and standards in integrating surveys of structural variation.
1042 *Nature Genetics*, 39(7), Article 7. <https://doi.org/10.1038/ng2093>
1043 Schloissnig, S., Pani, S., Rodriguez-Martin, B., Ebler, J., Hain, C., Tsapalou, V., Söylev, A., Hüther,
1044 P., Ashraf, H., Prodanov, T., Asparuhova, M., Hunt, S., Rausch, T., Marschall, T., & Korbel,
1045 J. O. (2024). *Long-read sequencing and structural variant characterization in 1,019*
1046 *samples from the 1000 Genomes Project* (p. 2024.04.18.590093). bioRxiv.
1047 <https://doi.org/10.1101/2024.04.18.590093>
1048 Smeds, L., Huson, L. S. A., & Ellegren, H. (2024). Structural genomic variation in the inbred
1049 Scandinavian wolf population contributes to the realized genetic load but is positively
1050 affected by immigration. *Evolutionary Applications*, 17(2), e13652.
1051 <https://doi.org/10.1111/eva.13652>
1052 Smit, A., Hubley, R., & Green, P. (2013). *RepeatMasker Open-4.0* (<http://www.repeatmasker.org>)
1053 [[Http://www.repeatmasker.org](http://www.repeatmasker.org)]. <http://www.repeatmasker.org>
1054 Soto, D. C., Uribe-Salazar, J. M., Shew, C. J., Sekar, A., McGinty, S. P., & Dennis, M. Y. (2023).
1055 Genomic structural variation: A complex but important driver of human evolution.
1056 *American Journal of Biological Anthropology*, 181 Suppl 76(Suppl 76), 118–144.
1057 <https://doi.org/10.1002/ajpa.24713>

1058 Spielmann, M., & Mundlos, S. (2016). Looking beyond the genes: The role of non-coding variants
1059 in human disease. *Human Molecular Genetics*, 25(R2), R157–R165.
1060 <https://doi.org/10.1093/hmg/ddw205>

1061 Stapley, J., Santure, A. W., & Dennis, S. R. (2015). Transposable elements as agents of rapid
1062 adaptation may explain the genetic paradox of invasive species. *Molecular Ecology*,
1063 24(9), 2241–2252. <https://doi.org/10.1111/mec.13089>

1064 Stuart, K. C., Edwards, R. J., Sherwin, W. B., & Rollins, L. A. (2023). Contrasting Patterns of Single
1065 Nucleotide Polymorphisms and Structural Variation Across Multiple Invasions.
1066 *Molecular Biology and Evolution*, 40(3), msad046.
1067 <https://doi.org/10.1093/molbev/msad046>

1068 Stuart, K. C., Santure, A. W., & Rollins, L. A. (2024). STRUCTURAL VARIANTS AND
1069 TRANSPOSABLE ELEMENTS AS FACILITATORS OF RAPID EVOLUTIONARY CHANGE IN
1070 INVASIVE POPULATIONS. In *Invasion Genomics*. In Review.

1071 Szarmach, S. J., Brelsford, A., Witt, C. C., & Toews, D. P. L. (2021). Comparing divergence
1072 landscapes from reduced-representation and whole genome resequencing in the
1073 yellow-rumped warbler (*Setophaga coronata*) species complex. *Molecular Ecology*,
1074 30(23), 5994–6005. <https://doi.org/10.1111/mec.15940>

1075 Tan, H. Z., Scherer, P., Stuart, K. C., Bailey, S., Lee, K. D., Brekke, P., Ewen, J. G., Whibley, A., &
1076 Santure, A. W. (2024). A high-density linkage map reveals broad- and fine-scale sex
1077 differences in recombination in the hihi (stitchbird; *Notiomystis cincta*). *Under Review*.

1078 Theissinger, K., Fernandes, C., Formenti, G., Bista, I., Berg, P. R., Bleidorn, C., Bombarely, A.,
1079 Crottini, A., Gallo, G. R., Godoy, J. A., Jentoft, S., Malukiewicz, J., Mouton, A., Oomen, R.
1080 A., Paez, S., Palsbøll, P. J., Pampoulie, C., Ruiz-López, M. J., Secomandi, S., ... Zammit,
1081 G. (2023). How genomics can help biodiversity conservation. *Trends in Genetics*, 39(7),
1082 545–559. <https://doi.org/10.1016/j.tig.2023.01.005>

1083 Turro, E., Astle, W. J., Megy, K., Gräf, S., Greene, D., Shamardina, O., Allen, H. L., Sanchis-Juan,
1084 A., Frontini, M., Thys, C., Stephens, J., Mapeta, R., Burren, O. S., Downes, K., Haimel, M.,
1085 Tuna, S., Deevi, S. V. V., Aitman, T. J., Bennett, D. L., ... Ouwehand, W. H. (2020). Whole-
1086 genome sequencing of patients with rare diseases in a national health system. *Nature*,
1087 583(7814), 96–102. <https://doi.org/10.1038/s41586-020-2434-2>

1088 Usha, T., Panda, P., Goyal, A. K., Kukanur, A. A., Kamala, A., Prasannakumar, M. K.,
1089 Sidhalinghamurthy, K., & Middha, S. K. (2022). Whole-Genome Sequencing of Plants:
1090 Past, Present, and Future. In R. L. Singh, S. Mondal, A. Parihar, & P. K. Singh (Eds.), *Plant*
1091 *Genomics for Sustainable Agriculture* (pp. 191–239). Springer Nature.
1092 https://doi.org/10.1007/978-981-16-6974-3_8

1093 Waters, P. D., Patel, H. R., Ruiz-Herrera, A., Álvarez-González, L., Lister, N. C., Simakov, O., Ezaz,
1094 T., Kaur, P., Frere, C., Grützner, F., Georges, A., & Graves, J. A. M. (2021).
1095 Microchromosomes are building blocks of bird, reptile, and mammal chromosomes.
1096 *Proceedings of the National Academy of Sciences*, 118(45), e2112494118.
1097 <https://doi.org/10.1073/pnas.2112494118>

1098 Weissensteiner, M. H., Bunikis, I., Catalán, A., Francoijs, K.-J., Knief, U., Heim, W., Peona, V.,
1099 Pophaly, S. D., Sedlazeck, F. J., Suh, A., Warmuth, V. M., & Wolf, J. B. W. (2020). Discovery
1100 and population genomics of structural variation in a songbird genus. *Nature*
1101 *Communications*, 11(1), 3403. <https://doi.org/10.1038/s41467-020-17195-4>

1102 Wellenreuther, M., Mérot, C., Berdan, E., & Bernatchez, L. (2019). Going beyond SNPs: The role
1103 of structural genomic variants in adaptive evolution and species diversification.
1104 *Molecular Ecology*, 28(6), 1203–1209. <https://doi.org/10.1111/mec.15066>

1105 Wold, J. R., Guhlin, J. G., Dearden, P. K., Santure, A. W., & Steeves, T. E. (2023). The promise and
1106 challenges of characterizing genome-wide structural variants: A case study in a critically
1107 endangered parrot. *Molecular Ecology Resources*, n/a(n/a).
1108 <https://doi.org/10.1111/1755-0998.13783>

1109 Wold, J. R., Koepfli, K.-P., Galla, S. J., Eccles, D., Hogg, C. J., Le Lec, M. F., Guhlin, J., Santure, A.
1110 W., & Steeves, T. E. (2021). Expanding the conservation genomics toolbox: Incorporating
1111 structural variants to enhance genomic studies for species of conservation concern.
1112 *Molecular Ecology*, 30(23), 5949–5965. <https://doi.org/10.1111/mec.16141>

1113 Yang, J., Li, W.-R., Lv, F.-H., He, S.-G., Tian, S.-L., Peng, W.-F., Sun, Y.-W., Zhao, Y.-X., Tu, X.-L.,
1114 Zhang, M., Xie, X.-L., Wang, Y.-T., Li, J.-Q., Liu, Y.-G., Shen, Z.-Q., Wang, F., Liu, G.-J., Lu,
1115 H.-F., Kantanen, J., ... Liu, M.-J. (2016). Whole-Genome Sequencing of Native Sheep
1116 Provides Insights into Rapid Adaptations to Extreme Environments. *Molecular Biology
1117 and Evolution*, 33(10), 2576–2592. <https://doi.org/10.1093/molbev/msw129>

1118 Zhao, S., Zheng, P., Dong, S., Zhan, X., Wu, Q., Guo, X., Hu, Y., He, W., Zhang, S., Fan, W., Zhu, L.,
1119 Li, D., Zhang, X., Chen, Q., Zhang, H., Zhang, Z., Jin, X., Zhang, J., Yang, H., ... Wei, F.
1120 (2013). Whole-genome sequencing of giant pandas provides insights into demographic
1121 history and local adaptation. *Nature Genetics*, 45(1), 67–71.
1122 <https://doi.org/10.1038/ng.2494>

1123